

1 ***PLoS Pathogens***

2

3

4 **An insect serotonin receptor mediates cellular immune responses**
5 **and its inhibition by phenylethylamide derivatives from bacterial**
6 **secondary metabolites**

7

8 **Md Ariful Hasan¹, Hyun-Suk Yeom², Jaewook Ryu², Helge B. Bode³, Yonggyun Kim^{1,*}**

9

10 ¹Department of Plant Medicals, College of Life Sciences, Andong National University, Andong
11 36729, Korea. ² Center for Eco-Friendly New Materials, Korea Research Institute of Chemicals
12 Technology, Yuseong, Daejeon 34114, Korea. ³ Department of Biosciences, Molecular
13 Biotechnology, and Buchmann Institute for Molecular Life Sciences (BMLS), Goethe-
14 Universität Frankfurt am Main, Germany

15

16 * Corresponding author: hosanna@anu.ac.kr

17

18

19

20 **Abstract**

21 Serotonin (5-hydroxytryptamine: 5-HT) is a biogenic monoamine that mediates immune
22 responses and modulates nerve signal in insects. *Se-5HTR*, a specific receptor of serotonin, has
23 been identified in the beet armyworm, *Spodoptera exigua*. It is classified into subtype 7 among
24 known 5HTRs. *Se-5HTR* was expressed in all developmental stages of *S. exigua*. It was
25 expressed in all tested tissues of larval stage. Its expression was up-regulated in hemocytes and
26 fat body in response to immune challenge. RNA interference (RNAi) of *Se-5HTR* exhibited
27 significant immunosuppression by preventing cellular immune responses such as phagocytosis
28 and nodulation. Treatment with an inhibitor (SB-269970) specific to 5HTR subtype 7 resulted in
29 significant immunosuppression. Such immunosuppression was also induced by bacterial
30 secondary metabolites derived from *Xenorhabdus* and *Photorhabdus*. To determine specific
31 bacterial metabolites inhibiting Se-5HTR, this study screened 37 bacterial secondary metabolites
32 with respect to cellular immune responses associated with Se-5HTR and selected 10 potent
33 inhibitors. These 10 selected compounds competitively inhibited cellular immune responses
34 against 5-HT and shared phenylethylamide (PEA) chemical skeleton. Subsequently, 46 PEA
35 derivatives were screened and resulting potent chemicals were used to design a compound to be
36 highly inhibitory against Se-5HTR. The designed compound was chemically synthesized. It
37 showed high immunosuppressive activities along with specific and competitive inhibition
38 activity for Se-5HTR. This study reports the first 5HT receptor from *S. exigua* and provides its
39 specific inhibitor designed from bacterial metabolites and their derivatives.

40

41 **Author Summary**

42 Serotonin (5-hydroxytryptamine: 5-HT) plays a crucial role in mediating nerve and immune
43 signals in insects. Interruption of 5-HT signal leads to malfunctioning of various insect
44 physiological processes. Se-5HTR, a 5-HT receptor of beet armyworm, *Spodoptera exigua*, was
45 identified and classified as subtype 7 (5-HT₇) of 5-HT receptors. A specific inhibitor (SB-269970)
46 for 5-HT₇ highly inhibited immune responses such as phagocytosis and nodulation mediated by
47 Se-5HTR. Two entomopathogenic bacteria, *Xenorhabdus* and *Photorhabdus*, could secrete
48 potent inhibitors against immune responses mediated by 5-HTR. Bacterial secondary metabolites
49 were screened against Se-5HTR-mediating immune responses. Most of resulting compounds
50 shared phenylethylamide (PEA) chemical skeleton. Subsequent screening using PEA derivatives
51 supported the importance of this chemical skeleton. Based on their relative inhibitory activities, a
52 compound was designed and synthesized. This novel compound possessed high inhibitory
53 activities against Se-5HTR-mediating immune responses and exhibited competitive inhibition
54 with 5-HT.

55

56 **Introduction**

57 Serotonin or 5-hydroxytryptamine (5-HT) is a biogenic monoamine found across most phyla of
58 life [1]. This indolamine compound is biosynthesized from tryptophan by successive catalytic
59 activities of tryptophan hydroxylase and aromatic-L-amino acid decarboxylase [2-4] primarily in
60 nervous systems [5,6]. In human and other vertebrates, serotonin is a well-known
61 neurotransmitter involved in mood, appetite, sleep, anxiety, cognition, and psychosis [7-9].
62 Outside the nervous system, serotonin plays important roles as growth factor and regulator of
63 hemostasis and blood clotting [10,11]. In plants, serotonin is basically involved in stress
64 signaling [12]. Serotonin plays crucial role in physiological and behavioral processes in insects
65 and other invertebrates [13,14]. In *Drosophila melanogaster*, there is evidence that serotonin is
66 required for courtship and mating [15], circadian rhythm [16,17], sleep [18], locomotion [13,19],
67 aggression [20], insulin signaling and growth [21], and phagocytosis [22]. Serotonin is also
68 involved in olfactory processing [23], feeding behavior [19], heart rate [24], and responses to
69 light [25] in *D. melanogaster* larvae.

70 Serotonin modulates physiological processes by binding to specific receptors. Seven main
71 subtypes of serotonin receptors have been classified in vertebrates [26]. Except 5-HT₃ receptor,
72 the other six classes (5-HT₁, 5-HT₂, 5-HT₄, 5-HT₅, 5-HT₆, and 5-HT₇ receptors) belong to G
73 protein-coupled receptor family [27]. Among these receptors, 5-HT₁ and 5-HT₅ receptors can
74 inhibit cAMP synthesis by preferentially coupling to a trimeric G protein G_{i/o} [28]. 5-HT₂
75 receptor uses G_{q/11} to induce breakdown of inositol phosphates, resulting in an increase in
76 cytosolic Ca²⁺ level [28]. Besides, 5-HT₄, 5-HT₆, and 5-HT₇ receptors coupled to G_s can
77 stimulate cAMP production [28]. However, 5-HT₃ receptor is a ligand-gated cation channel that
78 mediates neuronal depolarization [29].

79 Insects have at least three subtypes of 5-HT receptors. Five different 5-HT receptors as
80 orthologous to mammalian 5-HT_{1A}, 5-HT_{1B}, 5-HT_{2A}, 5-HT_{2B}, and 5-HT₇ have been identified in
81 *D. melanogaster* [14]. In addition, partial sequences of two 5-HT₁, two 5-HT₂, and one 5-HT₇
82 receptors have been identified in the field cricket *Gryllus bimaculatus* [30]. Two 5-HT₁ receptors
83 and two 5-HT₁ splice variants have been described in *Tribolium castaneum* and *Papilio xuthus*,
84 respectively [31,32]. As from *D. melanogaster* and *G. bimaculatus*, two 5-HT₂ receptors have
85 been described from *Apis mellifera* while only one 5-HT₂ receptor has been reported in other
86 insects such as *Periplaneta americana* and *Locusta migratoria* [33,34]. In a lepidopteran species,
87 *Pieris rapae*, four different 5-HT receptors including a novel subtype 8 have been reported
88 [35,36].

89 5-HT modulates various physiological processes via expression of different receptor types in
90 various tissues. 5-HT receptors are expressed highly in brain and ventral nerve cord of insects
91 [32]. 5-HT₁ receptor in honey bee brain is involved in visual information processing [37].
92 Expression pattern of 5-HT₇ receptor in honey bee nervous system suggests its possible roles in
93 information processing, learning, and memory [38]. 5-HT receptors might play roles in
94 neuroendocrine secretion and gut motility in cockroaches [29]. In salivary gland of several
95 insects, 5-HT₇ receptor has been reported to be involved in salivary secretion mediated by cAMP
96 level elevation [33,39,40]. Moreover, 5-HT₇ receptor mediates visceral muscle contraction in the
97 gastrointestinal tract of several insects including *A. aegypti* and *T. castaneum* [41,42]. 5-HT not
98 only has neurophysiological roles, but also mediates cellular immune responses in insects by
99 enhancing phagocytosis and nodulation [43]. Two different 5-HT receptors (1B and 2B) are
100 expressed in hemocytes of *P. rapae*, of which 5-HT receptor 1B mediates cellular immune
101 response [22]. In another lepidopteran insect, *Spodoptera exigua*, 5-HT mediates increase of total

102 circulatory hemocyte number by stimulating sessile hemocytes and mediating cellular immune
103 responses such as phagocytosis and nodule formation [44,45]. However, 5-HT receptor in *S.*
104 *exigua* has not been reported yet.

105 Two entomopathogenic bacteria, *Xenorhabdus* and *Photorhabdus*, can inhibit insect immune
106 responses to protect themselves and their symbiotic nematodes [46]. To accomplish host
107 immunosuppression, these bacteria can synthesize and secrete secondary metabolites to inhibit
108 immune signals and effectors [47]. Among these bacterial metabolites, tryptamine and
109 phenylethylamide derivatives have been identified with suggested function of interrupting 5-HT
110 signaling [48]. The objective of the present study was to determine bacterial secondary
111 compound(s) that could inhibit 5-HT signaling. To this end, we identified 5-HT receptor that
112 could mediate insect immunity in *S. exigua*. To determine a potent inhibitor of this receptor, we
113 screened bacterial secondary metabolites and their potent derivatives.

114

115 **Results**

116 **Bioinformatics analyses reveal that *S. exigua* contains a 5-HT receptor**

117 From a short read archive database (GenBank accession number: SRR1050532) of *S. exigua*, a
118 highly matched contig (accession number: GARL01017386.1) containing 3,308 bp nucleotide
119 sequence with an open reading frame (ORF) from 996th to 2,690th bp was identified. Prediction
120 of amino acid sequence by BlastP analysis revealed that its ORF sequence shared identities with
121 other insect 5-HT receptors: 99% with *Spodoptera litura* 5HTR (XP_022827337.1), 98% with
122 *Helicoverpa armigera* 5HTR (XP_021195909.1), 95% with *Trichoplusia ni* 5HTR
123 (XP_026729862.1), and 85% with *Manduca sexta* 5HTR (AGL46976.1). This novel 5-HT
124 receptor from *S. exigua* (Se-5HTR) encoded a sequence of 564 amino acids having a predicted

125 molecular weight of about 63.23 kDa. Phylogenetic analysis of its protein sequence indicated
126 that *Se-5HTR* was clustered with other 5-HT₇ receptors (Fig 1A). Predicted amino acid sequence
127 of *Se-5HTR* contained a signal peptide of 35 residues and attained GPCR character with seven
128 transmembrane domains. Consensus N-linked glycosylation sites are located in the N-terminus
129 (Asn⁴⁸ and Asn⁵³), the third intracellular loop (Asn³⁶²), and C-terminus (Asn⁵³⁴). Several
130 consensus sites for phosphorylation by protein kinase A and/or protein kinase C were predicted
131 throughout the length of the sequence. A disulfide bond between two Cys residues at
132 extracellular matrix ('ECM', S1 Fig) is also predicted.

133 *Se-5HTR* sequence attains highly conserved amino acid residues (Fig 1B) found uniquely in
134 the biogenic monoamine receptor family [49-51]. Negatively charged Asp residue in TM3
135 (Asp¹⁶³) might interact with positively charged amino group of the ligand. A hydrogen bond
136 between the hydroxyl group of serine residue in TM5 (Ser²⁴⁷) and the hydroxyl group of 5-HT
137 was predicted. In TM6, the consensus sequence unique to aminergic receptors (Phe⁴⁴⁴-X-X-X-
138 Trp⁴⁴⁸-X-Pro⁴⁵⁰-X-Phe⁴⁵²) is conserved. Like other GPCRs, a possible motif (Asn⁴⁸⁵-Pro⁴⁸⁶-X-X-
139 Tyr⁴⁸⁹) that might participate in agonist-mediated sequestration and re-sensitization of *Se-5HTR*
140 is conserved in TM7. The C-terminus of the receptor contains two potential post-translational
141 palmitoylation cysteine residues (Cys⁵⁰⁸ and Cys⁵³²) and PDZ (post synaptic density protein,
142 *Drosophila* disc large tumor suppressor, and zonula occludens-1 protein)-domain binding motif
143 (Glu⁵⁶¹-Ser⁵⁶²-Phe⁵⁶³-Leu⁵⁶⁴).

144

145 ***Se-5HTR* is expressed in all developmental stages and larval tissues**

146 Expression of *Se-5HTR* in different developmental stages of *S. exigua* was assessed by RT-PCR.
147 Results showed its expression from egg to adult stages (Fig 2A). RT-qPCR revealed variation in

148 its expression among developmental stages, with L5 larvae and adults showing the highest
149 expression levels. In L5 larvae, all tissues analyzed by RT-PCR showed its expression (Fig 2B).
150 RT-qPCR revealed that the midgut exhibited the highest expression level of *Se-5HTR*.
151 Hemocytes and brain also showed relatively high levels of its expression. Basal expression levels
152 of *Se-5HTR* were highly up-regulated in response to immune challenge (Fig 2C). *Se-5HTR*
153 expression was increased ~125-fold after challenge with fungus, *Beauveria bassiana* compared
154 to control (unchallenged). It was increased 60~90-fold after bacterial challenge compared to
155 naïve larvae.

156

157 **Specific inhibitors against 5-HT₇ suppress hemocyte behaviors of *S. exigua***

158 A commercial inhibitor (SB-269970) specific to 5-HT₇ was used to assess its effect on hemocyte
159 behaviors of *S. exigua* (Fig 3). Total hemocyte count (THC) of L5 larvae was $\sim 1.2 \times 10^7$
160 cells/mL (Fig 3A). THC was significantly ($P < 0.05$) increased in response to 5-HT or bacterial
161 challenge. SB-269970 prevented the increase of THC in response to bacterial challenge. Its IC₅₀
162 value was estimated to be 1.925 μ M. These results suggest that *Se-5HTR* can mediate hemocyte
163 mobilization in response to 5-HT upon bacterial challenge.

164 To determine the modulation effect of *Se-5HTR* on hemocyte-spreading behavior,
165 competitive inhibition between SB-269970 and 5-HT against *Se-5HTR* was assessed (Fig 3B).
166 Hemocytes were spread on slide glass with growth of F-actin. However, SB-269970 significantly
167 ($P < 0.05$) suppressed such hemocyte-spreading behavior. The inhibitory effect of the inhibitor
168 was rescued by addition of 5-HT. A relatively low dose (SB-269970: 5-HT = 10:1) of 5-HT did
169 not rescue the inhibitory effect. However, a relatively high dose (1:10) of 5-HT significantly ($P <$
170 0.05) rescued such inhibitory effect, indicating a specific competition between inhibitor and

171 ligand against Se-5HTR.

172

173 **RNA interference (RNAi) of Se-5HTR**

174 To address the immunomodulatory effect of Se-5HTR on hemocytes, its gene expression was
175 knocked-down by RNAi (Fig 4). RNAi was performed using dsRNA specific to *Se-5HTR*.
176 dsRNA-injected larvae exhibited significant ($P < 0.05$) reduction of *Se-5HTR* expression. RT-
177 qPCR analysis showed that about 90% of *Se-5HTR* mRNA was suppressed by dsRNA treatment
178 at 24 h PI (Fig 4A). At 24 h PI of dsRNA, *Se-5HTR* expression was analyzed in four different
179 tissue samples. Compared to control tissues, dsRNA-treated larvae exhibited significant ($P <$
180 0.05) reduction of *Se-5HTR* expression in all tissues including hemocytes.

181

182 **RNAi of Se-5HTR suppresses hemocyte behaviors of *S. exigua***

183 The effect of RNAi specific to Se-5HTR on hemocyte mobilization in response to bacterial
184 challenge was analyzed (Fig 4B). Upon bacterial challenge, THC increased by more than two
185 folds. However, RNAi treatment significantly ($P < 0.05$) suppressed such increase of THC. The
186 RNAi treatment also significantly ($P < 0.05$) influenced hemocyte-spreading behavior (Fig 4C).
187 On glass slide, hemocytes exhibited spreading behavior in 40 min by cytoskeletal rearrangement
188 through F-actin growth (see phalloidin staining). However, hemocytes collected from larvae
189 treated with RNAi specific to Se-5HTR lost such behavior.

190

191 **Modulation of cellular immune responses by Se-5HTR**

192 The influence of Se-5HTR on modulating hemocyte-spreading behavior suggested that it might
193 mediate cellular immune responses against bacterial infection. Phagocytosis against FITC-

194 labeled *Escherichia coli* was observed in hemocytes from control larvae. Labeled bacteria were
195 observed within hemocytes of control larvae (Fig 5A). However, hemocytes of larvae treated
196 with dsRNA specific to Se-5HTR significantly ($P < 0.05$) lost such phagocytosis, similar to that
197 found for hemocytes of larvae treated with SB-269970. Phagocytosis was decreased around 57%
198 or 78% after treatment with dsRNA or inhibitor, respectively. In response to bacterial challenge,
199 *S. exigua* formed ~78 hemocytic nodules per larva (Fig 5B). However, RNAi specific to Se-
200 5HTR or inhibitor treatment significantly ($P < 0.05$) reduced such cellular immune response.

201

202 **Influence of bacterial secondary metabolites on immune responses mediated by Se-5HTR**

203 RNAi or specific inhibitor assays indicated that 5-HTR could mediate both cellular immune
204 responses of phagocytosis and nodule formation in response to bacterial challenge. Bacterial
205 metabolites of two entomopathogens, *Xenorhabdus nematophila* (Xn) and *Photorhabdus*
206 *temperata temperata* (Ptt), were extracted from their culture broth using different organic
207 solvents and their inhibitory activities against cellular immune responses were then assessed (Fig
208 6). Organic solvent extracts of Xn- or Ptt-cultured broth exhibited significant ($P < 0.05$)
209 inhibitory activities against phagocytosis (Fig 6A) and nodulation (Fig 6B), although there were
210 variations in their inhibitory activities among extracts.

211 To identify bacterial secondary compounds that could inhibit Se-5HTR, 37 compounds (HB4
212 – HB602) derived from *Xenorhabdus* and *Photorhabdus* [47] were screened for their inhibitory
213 activities against hemocyte nodule formation and phagocytosis (Fig 7). More than three 75% (28
214 out of 37 compounds) of these test compounds exhibited significant ($P < 0.05$) inhibition against
215 phagocytosis (Fig 7A). In nodulation assay, all test compounds exhibited significant ($P < 0.05$)
216 inhibition (Fig 7B). Since Se-5HTR could mediate both cellular immune responses, bacterial

217 compounds that highly inhibited both phagocytosis (\square 60%) and nodulation (\square 30 nodules per
218 larva) were selected. As a result, 10 potent chemicals (HB 4, HB 5, H23, HB 30, HB44, HB 45,
219 HB 50, HB 223, HB 302, and HB 531) belonging to six chemical categories [phenylethylamide
220 (PEA), tryptamide, xenortide, xenocycloin, nematophin, and GameXPeptide] were found (S2
221 Fig). All these compounds exhibited median inhibitory concentration (IC_{50}) of 58~253 μ M
222 against cellular immune response of hemocytic nodulation.

223 To support the specific inhibitory activity of these selected compounds against Se-5HTR,
224 competitive assay was performed between test compounds and 5-HT (Fig 8). With a constant
225 concentration of 5-HT, phagocytotic behavior of *S. exigua* hemocytes gradually decreased with
226 increasing amount of test compound (Fig 8A). On the other hand, increase of 5-HT amount
227 gradually decreased the phagocytotic behavior using a constant amount of test compound (Fig
228 8B).

229

230 **Influence of PEA derivatives on phagocytosis mediated by Se-5HTR**

231 These 10 selected compounds shared phenyl (or aromatic) ethylamide backbone except
232 xenocycloin (S2 Fig). Based on PEA backbone, 45 derivatives were selected from a chemical
233 bank and their inhibitory activities against the phagocytotic behavior of *S. exigua* hemocytes
234 were tested (Fig 9A). More than 66% (30 out of 45 compounds) of PEA derivatives exhibited
235 significant ($P < 0.05$) inhibition against phagocytosis. Three PEA derivatives (Ph15, Ph17, Ph33)
236 had inhibitory activities similar to a bacterial metabolite (HB 44), with IC_{50} at 1.8 ~ 5.6 μ M
237 against phagocytosis (Fig 9B). These three PEA derivatives competitively inhibited the
238 phagocytosis mediated by Se-5HTR (Fig 9C).

239

240 **Synthesis of a potent inhibitor and inhibitory efficacy against Se-5HTR**

241 Potent compounds from 45 PEA derivatives were analyzed for their structures and activities
242 against phagocytosis mediated by Se-5HTR (S3 Fig). They shared the PEA backbone. However,
243 they had different side chains at 'X' and 'Y' (Fig S6A). When different X substituents were
244 compared for their inhibitory activities, methoxy was the most potent moiety (Fig S6B). When
245 different Y substituents were compared for their inhibitory activities with respect to identical X
246 groups, hexahydropyrrolo[1,2-a]pyrazine-1,4-dione was the most potent moiety (Fig S6C). This
247 analysis allowed us to design a hypothetical compound containing methoxy in X and
248 hexahydropyrrolo[1,2-a]pyrazine-1,4-dione at Y based on PEA backbone (Fig. S6D).

249 The designed compound ('PhX') was chemically synthesized and in its inhibitory activity
250 against phagocytosis was assessed compared with a specific 5-HT₇ inhibitor, SB269970, as a
251 reference (Fig 10). PhX was highly potent. It competitively inhibited cellular immune response
252 with 5-HT. Its inhibitory activity was more potent ($t = 14.9$; $df = 32$; $P \leq 0.0001$) than SB269970.

253

254 **Discussion**

255 5-HT plays a crucial role in mediating cellular immune responses of *S. exigua* by stimulating
256 actin rearrangement [45]. Furthermore, it performs a functional cross-talk with eicosanoid
257 signaling via a small G protein Rac1 [52]. However, its signaling pathway leading to immune
258 responses remains unclear due to the lack of its receptor information in *S. exigua*. This study
259 identified a 5-HT receptor and showed its physiological function in mediating immune responses.

260 Se-5HTR attains seven transmembrane domains and shares common molecular characters
261 with other 5-HT receptors. Like other GPCRs, Se-5HTR contains the canonical seven
262 transmembrane domains along with consensus glycosylation in the N-terminus (Asn⁴⁸ and Asn⁵³)

263 [53]. Additionally, its sequence contains a consensus aspartic acid residue in TM3 (Asp¹⁶³) and a
264 serine residue in TM5 (Ser²⁴⁷) to interact with functional groups of biogenic monoamines [54].
265 At the intracellular border of TM3, the highly conserved Asp¹⁸⁰-Arg¹⁸¹-Tyr¹⁸² motif is evident for
266 a strong ionic interaction with Glu⁴³⁰ residue adjacent to the intracellular end of TM6 that plays a
267 crucial role in GPCR signal transduction [55]. The sequence contains consensus Phe⁴⁴⁴-X-X-X-
268 Trp⁴⁴⁸-X-Pro⁴⁵⁰-X-Phe⁴⁵² motif in TM6 which is unique to biogenic monoamine GPCRs [38].
269 Additionally, *Se-HTR* contains two potential post-translational palmitoylation cysteine residues
270 (Cys⁵⁰⁸ and Cys⁵³²) [56] at the final intracellular region with a PDZ-domain binding motif
271 (Glu⁵⁶¹-Ser⁵⁶²-Phe⁵⁶³-Leu⁵⁶⁴) at the C-terminus [57].

272 *Se-5HTR* is expressed in all developmental stages. It is expressed in immune-associated
273 tissues (hemocytes and fat body), digestive (gut) tissues, and nervous (brain) tissues at larval
274 stage. Three 5-HT receptors of *P. rapae* larvae are all expressed, although their expression levels
275 in tissues are different. Subtypes 1A and 1B receptor are highly expressed in nervous tissues
276 while subtype 7 receptor is mainly expressed in digestive tissue [36]. *Se-5HTR* was also highly
277 expressed in the gut like 5-HT₇ of *P. rapae*. Furthermore, our phylogenetic analysis of 5-HT
278 receptors showed that these two insect 5-HT₇s were closely related and clustered. Expression
279 levels of *Se-5HTR* in hemocytes were similar to those in the brain. This suggests that *Se-5HTR* is
280 associated with immune function as well as neurophysiological function. Indeed, bacterial or
281 fungal infection up-regulated the expression of *Se-5HTR*. The increase of *Se-5HTR* expression
282 might be explained by the up-regulation of *de novo* biosynthesis of its ligand, 5-HT, via increase
283 in expression of biosynthetic genes as seen in hemocytes of *P. rapae* larvae after immune
284 challenge [22].

285 The presence of 5-HT₇ receptor in hemocytes of *S. exigua* and its physiological function
286 associated with immune responses were supported by its sensitivity to specific 5-HTR inhibitors.
287 In response to 5-HT or bacterial challenge, *S. exigua* larvae exhibited significant increase of
288 THC. This up-regulation of THC was explained by mobilization of sessile hemocytes to
289 circulatory form by cytoskeletal rearrangement via a small G protein, Rac1 [45,52]. This
290 suggests that Se-5HTR can activate Rac1 to stimulate the hemocyte behavior. In vertebrates,
291 activation of 5-HT₇ receptor increases cAMP level via a trimeric G protein G_s and small G
292 proteins of Rho family including Cdc42, RhoA, and Rac1 via another trimeric G protein G₁₂ [58].
293 This suggests that immune challenge can induce biosynthesis and release of 5-HT which then
294 binds to Se-5HTR on hemocytes and activates Rac1 to stimulate hemocyte behaviors. In addition,
295 the cAMP pathway triggered by Se-5HTR might activate Akt and ERK1/2 as seen in mammalian
296 cancer cells [59] to facilitate actin rearrangement to form cellular shape change of hemocytes.
297 These findings suggest that Se-5HTR plays a crucial role in hemocyte migration and cell shape
298 change during cellular immune responses. Indeed, RNAi of *Se-5HTR* expression resulted in
299 significant immunosuppression by exhibiting reduction in phagocytosis and nodulation.

300 Bacterial metabolites derived from two entomopathogens, *Xenorhabdus* and *Photorhabdus*,
301 inhibited cellular immune responses mediated by Se-5HTR. Especially, six chemical groups
302 (phenylethylamide, tryptamide, xenortide, xenocycloin, nematophin, and GameXPeptide) highly
303 inhibited both phagocytosis and nodulation, suggesting that they can inhibit Se-5HTR. This was
304 supported by their competitive inhibition with the ligand, 5-HT. Bacterial secondary metabolites
305 may be synthesized and released in the bacterium-nematode complex in order to defend immune
306 attack from target insect to compete with other microbes occurring in the insect cadaver and
307 facilitate host nematode development or bacterial quorum sensing [47]. It has been reported

308 phenylethylamides and tryptamides identified from *Xenorhabdus* can act as quorum quenching
309 activators by competitive binding to N-acylated homoserine lactone (AHL) receptor because
310 AHL accumulation drives gene expression of bioluminescence, virulence factor, and biofilm
311 formation in bacteria [60,61]. Xenortides are linear peptides consisting of 2-8 amino acids
312 synthesized from both *Xenorhabdus* and *Photorhabdus* [62]. They are synthesized in insect hosts
313 during infection with putative role in inhibiting prophenoloxidase activation to suppress insect
314 immunity [63]. Xenocycloins produced by *X. bovienii* are cytotoxic to hemocytes of *Galleria*
315 *melonella* [64]. Nematophin is synthesized by condensation of α -keto acid and tryptamine in *X.*
316 *nematophila*. It possesses a specific antibacterial activity against *Staphylococcus aureus* [65].
317 GameXPeptides are cyclic pentapeptides widely synthesized in both *Xenorhabdus* and
318 *Photorhabdus*. However, their biological functions remain unclear [66]. This current study
319 showed that these six compound classes could inhibit cellular immune responses by competitive
320 inhibition with 5-HT against Se-5HTR.

321 A novel phenylethylamide compound, PhX, was found to be highly inhibitory against Se-
322 5HTR. Derivatives of phenylethylamide compound (HB 4) exhibited different inhibitory
323 activities against cellular immune responses mediated by Se-5HTR. Especially, PhX containing
324 methoxy and hexahydropyrrolo[1,2-a]pyrazine-1,4-dione exhibited the highest inhibitory activity.
325 5-HT receptors have been used for screening for potent insecticides with growth-inhibiting or
326 larvicidal activities against *Pseudaletia separata* [67]. Thus, PhX can be a candidate for this
327 application unless it shows mammalian or non-target species toxicity [68].

328

329 **Materials and methods**

330 **Insect rearing and microbial culture**

331 A laboratory strain of *S. exigua* was originated from Welsh onion field (Andong, Korea) and
332 maintained for ~20 years. Larvae of this laboratory strain were reared on an artificial diet [69] at
333 temperature of $25 \pm 1^\circ\text{C}$ and relative humidity of $60 \pm 10\%$ with a photoperiod of 16:8 h (L:D).
334 Under these conditions, larvae had five instars ('L1-L5'). Adults were reared with 10% sucrose
335 solution. For immune challenge, *Escherichia coli* Top10 (Invitrogen, Carlsbad, CA, USA) was
336 cultured in Luria-Bertani (LB) medium (BD Korea, Seoul, Korea) in a shaking incubator (200
337 rpm) at 37°C overnight (16 h).

338

339 **Chemicals**

340 Serotonin hydrochloride was purchased from Sigma-Aldrich Korea (Seoul, Korea). It was
341 dissolved in distilled water. SB-269970 (a specific inhibitor to 5-HT receptor subtype 7, 5-HT₇)
342 was purchased from Cayman Chemical Company (Korea). It was dissolved in desired
343 concentrations with dimethyl sulfoxide (DMSO). Fluorescein isothiocyanate (FITC) [2-(6-
344 hydroxy-3-oxo-3h-xanthen-9-yl)-5-isothiocyanatobenzoic acid] was purchased from Sigma-
345 Aldrich Korea. It was dissolved in DMSO to make a solution at 10 mg/mL. Anticoagulant buffer
346 (ACB) was prepared using 98 mM NaOH, 186 mM NaCl, 17 mM Na₂EDTA, and 41 mM citric
347 acid at pH 4.5. Phosphate-buffered saline (PBS) was prepared at pH 7.4 with 50 mM sodium
348 phosphate and 0.7% NaCl. Tris-buffered saline (TBS) was prepared using 150 mM NaCl, 50 mM
349 Tris-HCl at pH 7.6. Hank's balanced salt solution (HBSS) was prepared with the following
350 compositions: 8 g NaCl, 400 mg KCl, 40 mg Na₂HPO₄, 60 mg KH₂PO₄, 1 g glucose, 140 mg
351 CaCl₂, 120 mg MgSO₄, and 350 mg NaHCO₃ in 1,000 mL distilled H₂O.

352

353 **Bioinformatics to search for 5-HT receptor and sequence analysis**

354 *S. exigua* 5-HT receptor (Se-5HTR) sequence was obtained from GenBank by manual annotation.
355 Briefly, a dopamine receptor sequence (AKR18180.1) of *Chilo suppressalis* was used to screen a
356 transcriptome (SRR1050532) of *S. exigua*. A blast contig (GARL01017386.1) was analyzed for
357 open reading frame (ORF) and the predicted amino acid sequence was used for analysis using
358 BlastP program against GenBank (www.ncbi.nlm.nih.gov). After confirming its high homologies
359 (E value < 10⁻²⁰) with other known insect 5HTRs, the resulting ORF sequence (= Se-5HTR) was
360 deposited at NCBI-GenBank (accession number: MH025798). Sequence alignment was
361 established using Clustal Omega tool (<https://www.ebi.ac.uk/Tools/msa/clustalo/>) provided by
362 European Bioinformatics Institution. Phylogenetic tree was generated with Neighbor-joining
363 method using Mega6 and ClustalW programs. Bootstrapping values were obtained with 1,000
364 repetitions to support branch and clustering. Protein domain was predicted using InterPro tool
365 (<https://www.ebi.ac.uk/interpro/>), pfam (<http://pfam.xfam.org>), and Prosite
366 (<http://prosite.expasy.org/>).

367

368 **RNA extraction and cDNA preparation**

369 Using Trizol reagent (Invitrogen), total RNAs were extracted from all developmental stages as
370 well as larval tissues (hemocyte, midgut, fat body, and brain) of *S. exigua* according to the
371 instruction of the manufacturer. Numbers of individuals used for RNA extraction for each
372 individual developmental stage were as follows: ~500 eggs, ~20 larvae for L1-L2, ~10 larvae for
373 L3, ~5 larvae for L4, one larva for L5, one pupa, and one adult. L5 larvae were used for RNA
374 extraction from different tissue samples. After extraction, total RNAs were resuspended in
375 nuclease-free water and cDNAs were synthesized from ~1 µg of RNAs using Maxime RT
376 Premix (Intron Biotechnology, Seoul, Korea) according to the manufacturer's instruction.

377

378 **Expression pattern of *Se-5HTR* by RT-qPCR**

379 A fragment of *Se-5HTR* was amplified with gene-specific primers (5'- CTT TAC CTT CGT
380 GTC TTC TC-3' and 5'- GGT GTC AGT CTT CTC ATT AC -3'). PCR was performed with
381 35 cycles of denaturation (94°C, 1 min), annealing (49°C, 1 min), and extension (72°C, 1 min).
382 PCR products were subjected to agarose gel electrophoresis to visually confirm their
383 amplifications. With the same gene-specific primers used in RT-PCR, RT-qPCR was performed
384 in a qPCR machine (CFX Connect™ Real-Time PCR Detection System, Bio-Rad, Hercules, CA,
385 USA) using SYBR Green Realtime PCR Master Mix (Toyobo, Osaka, Japan) under a guideline
386 of Bustin et al. [70]. The amplification used 40 cycles of 15 s at 95°C, 30 s at 60°C, and 45 s at
387 72°C. After PCR reactions, melting curves from 60 to 95°C were obtained to confirm unique
388 PCR products. A ribosomal protein, RL32, gene was used as a control with primers of 5'-ATG
389 CCC AAC ATT GGT TAC GG-3' and 5'-TTC GTT CTC CTG GCT GCG GA-3'. Each
390 treatment was independently triplicated. Relative quantitative analysis method ($2^{-\Delta\Delta CT}$) was used
391 to estimate mRNA expression levels of *Se-5HTR*.

392

393 **RNA interference (RNAi)**

394 Gene fragment of *Se-5HTR* was amplified from template DNA using gene-specific primers (5'-
395 CTT TAC CTT CGT GTC TTC TC-3' and 5'-GGT GTC AGT CTT CTC AT-3') possessing T7
396 RNA polymerase promoter sequence (5'-TAA TAC GAC TCA CTA TAG GGA GA-3') at 5'
397 ends. PCR was performed with 5 cycles of denaturation (94°C, 1 min), annealing (49°C, 1 min),
398 and extension (72°C, 1 min) followed by 30 cycles of denaturation (94°C, 1 min), annealing
399 (60°C, 1 min), and extension (72°C, 1 min) to synthesize DNA template for dsRNA synthesis.

400 Double-stranded RNA (dsRNA) against *Se-5HTR* ('dsSe-5HTR') was synthesized using
401 Megascript RNAi kit (Ambion, Austin, TX, USA) following the manufacturer's instruction. The
402 resulting dsRNA was blended with Metafectene PRO (Biontex, Plannegg, Germany) at 1:1 (v:v)
403 ratio and incubated at 25°C for 30 min for liposome formation. Two microliters of the prepared
404 mixture containing ~900 ng of dsRNA was injected twice into *S. exigua* larval hemocoel using a
405 microsyringe (Hamilton, Reno, NV, USA) equipped with a 26-gauge needle. The first injection
406 was at late L4 stage. It was repeated 12 h afterwards. RNAi efficacy at 0, 24, and 48 h post-
407 injection (PI) in reducing *Se-5HTR* expression was determined by RT-qPCR. At 24 h PI, treated
408 larvae were used for immune challenge experiments. Each treatment was replicated thrice using
409 10 larvae for each replication.

410

411 **Total hemocyte count (THC)**

412 Hemolymph was collected by cutting larval proleg and mixed with ACB (1:10, v/v). Hemocytes
413 were counted using a Neubauer hemocytometer (Superior Marienfeld, Lauda-Königshofen,
414 Germany) under a phase contrast microscope (BX41, Olympus, Tokyo, Japan) at 100×
415 magnification. Heat-killed (90°C, 30 min) *Escherichia coli* (5×10^5 cells/larva) and a test
416 chemical (5-HT or SB-269970) were co-injected into hemocoel through abdominal proleg of L5
417 larvae in a volume of 5 µL using a 10 µL micro-syringe (Hamilton) after surface-sterilization
418 with 70% ethanol. After 4 h of incubation at $25 \pm 2^\circ\text{C}$, hemolymph of the insect was collected
419 and assessed for THC.

420

421 **Hemocyte-spreading analysis**

422 After hemolymph (~150 µL) was collected from five L5 larvae by cutting prolegs, it was mixed

423 with three times volume of ice-cold ACB and incubated on ice for 30 min. ACB-treated
424 hemolymph was then centrifuged at $800 \times g$ for 5 min at 4°C . The resulting pellet was re-
425 suspended in 500 μL of filter-sterilized TC-100 insect cell culture medium (Welgene, Daegu,
426 Korea). On a glass coverslip placed in a moist chamber, 10 μL of hemocyte suspension was
427 applied and placed in a dark condition. Hemocytes were then fixed with 4% paraformaldehyde
428 (filter-sterilized) at 25°C for 10 min and then washed thrice with filter-sterilized PBS. Cells were
429 then permeabilized with 0.2% Triton-X dissolved in PBS at 25°C for 2 min and washed with
430 PBS. After that, hemocytes were blocked using 10% bovine serum albumin (BSA) dissolved in
431 PBS at 25°C for 10 min and washed again with PBS. Cells were then incubated with FITC-
432 tagged phalloidin in PBS for 60 min and washed thrice with PBS. Hemocytes nuclei were then
433 stained by incubating with 4',6-diamidino-2-phenylindole (DAPI, 1 $\mu\text{g}/\text{mL}$) (Thermo Fisher
434 Scientific, Rockford, IL, USA) dissolved in PBS and washed thrice with PBS. Hemocytes were
435 then observed under a fluorescence microscope (DM2500, Leica, Wetzlar, Germany) at $400\times$
436 magnification. Hemocyte-spreading was dictated by appendages of F-actin outward the
437 hemocyte cell boundary.

438 To assess effect of *Se-5HTR* RNAi on hemocyte-spreading, hemocytes were collected at 24 h
439 after injecting ds*Se-5HTR* (~900 ng/larva). In separate experiments, 5-HT and 5-HTR inhibitor
440 SB-269970 were co-injected into dsRNA-treated larvae at ratios of 1:10 and 10:1 to check their
441 influence on hemocyte-spreading. At 6 h after co-injection, hemolymph was collected from the
442 treated larva and hemocyte-spreading was observed using the above-mentioned method.

443

444 **Nodulation assay**

445 Overnight culture of *E. coli* Top10 bacterial cells was washed with PBS and centrifuged at 1,120

446 $\times g$ for 10 min. L5 larvae were used to assess hemocyte nodule formation by immune-challenge
447 with bacterial injection ($\sim 1.8 \times 10^5$ cells/larva) through the abdominal proleg into larval
448 hemocoel using a microsyringe as previously described. To assess the effect of *Se-5HTR* RNAi
449 on nodule formation, bacterial challenge was performed at 24 h after injecting ds*Se-5HTR* (~ 900
450 ng/larva). To check the influence of chemicals on nodule formation, 2 μg of ketanserin and/or 10
451 μg of 5-HT was co-injected along with the bacterial suspension. In separate experiment, 1 μg of
452 the bacterial secondary metabolite was co-injected with the bacterial suspension to assess
453 immune suppression activity of the test compound. After an incubation period of 8 h at 25°C,
454 treated insects were dissected under a stereo microscope (SZX9, Olympus, Japan) to count
455 melanized nodule numbers. Each treatment was triplicated independently using five insects for
456 each replication.

457

458 **Phagocytosis assay**

459 Preparation of FITC-labeled bacterial cells followed the method described by Harlow and Lane
460 (1998). Briefly, *E. coli* Top10 cells were cultured in 50 mL of Luria-Bertani broth (37°C, 16 h).
461 These bacterial cells were then harvested by centrifuging 1 mL of the cultured broth at $1,120 \times g$
462 for 10 min at 4°C. Bacterial cells (10^5 cells/mL) were washed twice with TBS and re-suspended
463 in 1 mL of 0.1 M sodium bicarbonate buffer (pH 9.0). In the suspension, 1 μL of 10 mg/mL
464 FITC solution was added and immediately mixed. The mixture was then incubated under
465 darkness with end-over-end rotation at 25°C for 30 min. After the incubation, FITC-tagged
466 bacteria were harvested by centrifugation at $22,000 \times g$ for 20 min at 4°C. These bacterial cells
467 were washed thrice with HBSS to remove unbound dye and re-suspended in TBS.

468 To assess *in vivo* phagocytosis activity, 5 μL of FITC-tagged *E. coli* suspension was injected

469 into the hemocoel of L5 larva through the proleg. To assess the effect of *Se-5HTR* RNAi on
470 phagocytosis activity, bacteria were injected at 24 h after injecting ds*Se-5HTR* (~900 ng/larva).
471 To check the influence of a specific 5-HT₇ receptor inhibitor on phagocytosis, 2 µg of SB-
472 269970 was co-injected with the tagged bacterial suspension. To determine the effect of
473 secondary metabolite on phagocytosis, 1 µg of bacterial secondary metabolite was co-injected
474 with tagged bacterial suspension. After 15 min of incubation, treated larvae were surface-
475 sterilized using 70% ethanol. With a pair of scissors, the proleg was cut to collect hemolymph
476 sample (~50 µL) in 150 µL of cold ACB with gentle shaking of the tube to mix hemolymph and
477 ACB thoroughly. Hemocyte monolayers were made using 50 µL of hemocyte suspension (~5 ×
478 10³ cells) and left in a moist chamber for 15 min for hemocytes to settle and attach to the glass
479 surface. After the incubation period, monolayers were washed with TBS to remove plasma.
480 These monolayers were overlaid with 1% trypan blue dye solution to quench non-phagocytosed
481 bacterial cells. After 10 min, monolayers were washed again with TBS and then fixed with 1.5%
482 glutaraldehyde solution to observe under a fluorescence microscope at 400× magnification.
483 Hemocytes undergoing phagocytosis were counted from a total of 100 hemocytes observed from
484 different areas of each slide. Each observation was triplicated with three different slides.

485

486 **Preparation of organic extracts from bacterial culture broth**

487 *X. nematophila* K1 (Xn) and *P. temperate temperata* ANU101 (Pt) bacteria were cultured in
488 TSB at 28°C for 48 h. Culture broths were centrifuged at 12,500 × g for 30 min and supernatants
489 were used for subsequent fractionation. To obtain ethyl acetate extract, the same volume (1 L) of
490 ethyl acetate was mixed with the supernatant and separated into organic and aqueous fractions.
491 Ethyl acetate extract ('EAX') was dried using a rotary evaporator (Sunil Eyela, Seongnam,

492 Korea) at 40°C. The resulting extract (0.2 mg) was obtained from 1 L cultured broth and
493 resuspended with 5 mL of methanol. The aqueous phase was then combined with 1 L of butanol.
494 Butanol extract ('BX') was also dried using the rotary evaporator at 40°C and the resulting
495 extract (0.2 mg) was resuspended with 5 mL of methanol.

496

497 **Secondary bacterial metabolites – biological activity against immune responses**

498 Secondary metabolites (37 samples, S4 Fig) derived from *Xenorhabdus* and *Photorhabdus*
499 cultures were from the Bode lab compound collection named 'HB' compounds. Their biological
500 activities for suppressing *S. exigua* immunity were then determined. Individual chemicals were
501 dissolved in DMSO, diluted into desired concentrations with DMSO, and stored at -20°C.

502 For hemocyte nodulation inhibition assay, overnight culture of *E. coli* bacterial cells was
503 washed with PBS. Test compound (1 µg/larva) was injected into larval hemocoel along with the
504 bacterial suspension ($\sim 1.8 \times 10^5$ cfu/larva) using a microsyringe as previously described. Insects
505 were then incubated at 25°C for 8 h. After the incubation period, insects were dissected and
506 nodule numbers were counted as described above. Each treatment was triplicated independently
507 using five insects for each replication. For phagocytosis inhibition assay, 5 µL of FITC-tagged *E.*
508 *coli* suspension along with 1 µg of test compound was injected into L5 larval hemocoel. After 15
509 min of incubation period, hemocytes undergoing phagocytosis were counted as previously
510 described.

511

512 **Secondary bacterial metabolites – competitive assay with 5-HT**

513 To determine effects of bacterial secondary metabolites on nodulation and phagocytosis, 10
514 potent chemicals were selected based on their common inhibitory activity on both phagocytosis

515 and nodulation and their median inhibition concentration (IC₅₀) values were calculated.
516 Percentages of phagocytosis against increasing concentrations of HB chemicals were calculated
517 and their IC₅₀ values were calculated using Probit analysis (<https://probitanalysis.wordpress.com>).
518 To assess a competitive inhibitory activity between test compound and 5-HT, HB chemicals were
519 injected in different doses (0, 0.01, 0.1, 1 and 10 µg/larva) along with a fixed 5-HT concentration
520 (1 µg/larva) and FITC-tagged bacteria (500 cells/larva). In a separate experiment, different doses
521 of 5-HT were injected into the larvae with a fixed HB compound content (1 µg/larva). At 15 min
522 after bacterial injection, hemocytes from treated larvae were collected in ACB and phagocytosis
523 assay was performed as described above.

524

525 **Chemical derivatives and their inhibitory activities against Se-5HTR**

526 Based on potent phenylethylamide (PEA) HB compounds, 45 additional PEA samples (S5 Fig)
527 were obtained from Korea Chemical Bank of the Korea Research Institute of Chemical
528 Technology (KRICT). Derivative compounds were dissolved in DMSO, diluted into desired
529 concentrations with DMSO, and stored at -20°C. These PEA chemicals were then tested for their
530 abilities to suppress nodule formation and phagocytosis in *S. exigua* as described above. For
531 nodulation inhibition assay, each chemical (150 ng/larva) was injected into larval hemocoel
532 along with bacterial suspension ($\sim 1.8 \times 10^5$ cfu/larva). Each treatment was triplicated
533 independently using five insects for each replication. For phagocytosis inhibition assay, 5 µL of
534 FITC-tagged *E. coli* suspension along with 150 ng of each chemical was injected into L5 larval
535 hemocoel of *S. exigua*. After incubating for 15 min, hemocytes undergoing phagocytosis were
536 counted using previously described method.

537

538 **Chemical synthesis of PhX**

539 A potent chemical was designed as PhX ((*S*)-2-(1,4-dioxohexahydropyrrolo[1,2-*a*]pyrazin-
540 2(*1H*)-yl)-*N*-(4-methoxyphenethyl)acetamide) and chemically synthesized according to a method
541 described in S6 Fig.

542

543 **Statistical analysis**

544 All studies were triplicated independently. Results are expressed as mean \pm standard error.
545 Results were plotted using Sigma plot (Systat Software, San Jose, CA, USA). Means were
546 compared by least squared difference (LSD) test of one-way analysis of variance (ANOVA)
547 using POC GLM of SAS program [71] and discriminated at Type I error = 0.05.

548

549 **Funding**

550 This work was supported by a grant (No. 2017R1A2133009815) of the National Research
551 Foundation (NRF) funded by the Ministry of Science, ICT and Future Planning, Republic of
552 Korea. This work was also supported by a project (No SI1808, Development of crop protection
553 agents leading the future market). The chemical library used in this research was provided by
554 Korea Chemical Bank (<http://www.chembank.org>) of the Korea Research Institute of Chemical
555 Technology (KRICT).

556

557 **Acknowledgments**

558 We appreciate Youngim Song for ordering and arranging materials and Malsook Cho for rearing
559 insects. Work in the Bode lab was supported by the LOEWE Center Translational Biodiversity
560 Genomics funded by the state of Hesse, Germany.

561

562 **Author Contributions**

563 **Conceptualization:** Yonggyun Kim.

564 **Formal analysis:** Ariful Hasan, Yonggyun Kim.

565 **Investigation:** Hyun-Suk Yeom, Jaewook Ryu, Helge B. Bode, Yonggyun Kim.

566 **Project administration:** Yonggyun Kim.

567 **Supervision:** Hyun-Suk Yeom, Jaewook Ryu, Helge B. Bode, Yonggyun Kim.

568 **Writing – original draft:** Ariful Hasan, Yonggyun Kim.

569 **Writing – review & editing:** Ariful Hasan, Hyun-Suk Yeom, Jaewook Ryu, Helge B. Bode,

570 Yonggyun Kim.

571

572 **References**

573

574 1. Roshchina VV. 2010. New trends and perspectives in the evolution of neurotransmitters in
575 microbial, plant, and animal cells. *Adv Exp Med Biol.* 2016;874:25-77.

576 2. Lovenberg W, Weissbach H, Udenfriend S. 1962. Aromatic L-amino acid decarboxylase. *J*
577 *Biol Chem.* 1962;237:89-93.

578 3. Hufton SE, Jennings IG, Cotton RG. Structure and function of the aromatic amino acid
579 hydroxylases. *Biochem. J.* 1995;311:353-66.

580 4. Roberts KM, Fitzpatrick PF. 2013. Mechanisms of tryptophan and tyrosine hydroxylase.
581 *IUBMB Life* 2013;65:350-357.

582 5. Zhang X, Beaulieu JM, Sotnikova TD, Gainetdinov RR, Caron MG. Tryptophan
583 hydroxylase-2 controls brain serotonin synthesis. *Science.* 2004;305:217.

584 6. Gershon MD, Tack J. The serotonin signaling system: from basic understanding to drug
585 development for functional GI disorders. *Gastroenterology.* 2007;132:397-414.

586 7. Richtand NM, McNamara RK. Serotonin and dopamine interactions in psychosis prevention.
587 *Prog Brain Res.* 2008;172:141-53.

588 8. Monti JM. Serotonin control of sleep-wake behavior. *Sleep Med Rev.* 2011;15:269-81.

589 9. Švob Štrac D, Pivac N, Mück-Šeler D. The serotonergic system and cognitive function.
590 *Transl Neurosci.* 2016;7:35-49.

591 10. Seuwen K, Pouysségur J. Serotonin as a growth factor. *Biochem. Pharmacol.* 1990;39:985-90.

592 11. Li N, Wallén NH, Ladjevardi M, Hjemdahl P. Effects of serotonin on platelet activation in
593 whole blood. *Blood Coagul Fibrinolysis* 1997;8:517-23.

594 12. Hayashi K, Fujita Y, Ashizawa T, Suzuki F, Nagamura Y, Hayano-Saito Y. Serotonin

- 595 attenuates biotic stress and leads to lesion browning caused by a hypersensitive response to
596 *Magnaporthe oryzae* penetration in rice. *Plant J.* 2016;85:46-56.
- 597 13. Majeed ZR, Abdeljaber E, Soveland R, Cornwell K, Bankemper A, Koch F, et al. Modulatory
598 action by the serotonergic system: behavior and neurophysiology in *Drosophila*
599 *melanogaster*. *Neural Plast.* 2016;2016:1-23.
- 600 14. Huser A, Eschment M, Güllü N, Kan C, Böpple K, Pankevych L. et al. Anatomy and
601 behavioral function of serotonin receptors in *Drosophila melanogaster* larvae. *PLoS One*
602 2017;12:e0181865.
- 603 15. Becnel J, Johnson O, Luo J, Nässel DR, Nichols CD. The serotonin 5-HT_{7Dro} receptor is
604 expressed in the brain of *Drosophila*, and is essential for normal courtship and mating. *PLoS*
605 *One* 2011;6:e20800.
- 606 16. Yuan Q, Lin F, Zheng X, Sehgal A. Serotonin modulates circadian entrainment in *Drosophila*.
607 *Neuron.* 2005;47:115-27.
- 608 17. Nichols CD. 5-HT₂ receptors in *Drosophila* are expressed in the brain and modulate aspects
609 of circadian behaviors. *Dev Neurobiol.* 2007;67:752-63.
- 610 18. Yuan Q, Joiner WJ, Sehgal A. A sleep-promoting role for the *Drosophila* serotonin receptor
611 1A. *Curr. Biol.* 2006;16:1051-62.
- 612 19. Neckameyer WS, Coleman CM, Eadie S, Goodwin SF. Compartmentalization of neuronal
613 and peripheral serotonin synthesis in *Drosophila melanogaster*. *Genes Brain Behav.*
614 2007;6:756-69.
- 615 20. Dierick HA, Greenspan RJ. Serotonin and neuropeptide F have opposite modulatory effects
616 on fly aggression. *Nat. Genet.* 2007;39:678-82.
- 617 21. Kaplan DD, Zimmermann G, Suyama K, Meyer T, Scott MP. A nucleostemin family GTPase,

- 618 NS3, acts in serotonergic neurons to regulate insulin signaling and control body size. *Genes*
619 *Dev.* 2008;22:1877-93.
- 620 22. Qi YX, Huang J, Li MQ, Wu YS, Xia RY, Ye GY. Serotonin modulates insect hemocyte
621 phagocytosis via two different serotonin receptors. *Elife* 2016;5:e12241.
- 622 23. Python F, Stocker RF. Immunoreactivity against choline acetyltransferase, gamma-
623 aminobutyric acid, histamine, octopamine, and serotonin in the larval chemosensory system
624 of *Drosophila melanogaster*. *J. Comp. Neurol.* 2002;453:157-67.
- 625 24. Dasari S, Cooper RL. Direct influence of serotonin on the larval heart of *Drosophila*
626 *melanogaster*. *J. Comp. Physiol. B* 2006;176:349-57.
- 627 25. Rodriguez MVG, Campos AR. Role of serotonergic neurons in the *Drosophila* larval
628 response to light. *BMC Neurosci.* 2009;10:66.
- 629 26. Barnes, N.M., Sharp, T., 1999. A review of central 5-HT receptors and their function.
630 *Neuropharmacology* 38, 1083-1152.
- 631 27. Nichols DE, Nichols CD. Serotonin receptors. *Chem Rev.* 2008;108:1614-41.
- 632 28. Roth BL. The serotonin receptors: from molecular pharmacology to human therapeutics.
633 Humana Press, Totowa, New Jersey. 2006.
- 634 29. Thompson AJ, Lummis SCR. 5-HT₃ Receptors. *Curr. Pharm. Des.* 2006;12:3615-30.
- 635 30. Watanabe T, Sadamoto H, Aonuma H. Identification and expression analysis of the genes
636 involved in serotonin biosynthesis and transduction in the field cricket *Gryllus bimaculatus*.
637 *Insect Mol Biol.* 2011;20:619-35.
- 638 31. Ono H, Yoshikawa H. Identification of amine receptors from a swallowtail butterfly, *Papilio*
639 *xuthus* L.: cloning and mRNA localization in foreleg chemosensory organ for recognition of
640 host plants. *Insect Biochem Mol Biol.* 2004;34:1247-56.

- 641 32. Vleugels R, Lenaerts C, Baumann A, Vanden BJ, Verlinden H. Pharmacological
642 characterization of a 5-HT₁-type serotonin receptor in the red flour beetle, *Tribolium*
643 *castaneum*. PLoS One 2013;8:e65052.
- 644 33. Troppmann B, Balfanz S, Baumann A, Blenau W. Inverse agonist and neutral antagonist
645 actions of synthetic compounds at an insect 5-HT₁ receptor. Br. J. Pharmacol.
646 2010;159:1450-62.
- 647 34. Guo X, Ma Z, Kang L. Serotonin enhances solitariness in phase transition of the migratory
648 locust. Front. Behav Neurosci. 2013;7:129.
- 649 35. Qi YX, Xia RY, Wu YS, Stanley D, Huang J, Ye GY. Larvae of the small white butterfly,
650 *Pieris rapae*, express a novel serotonin receptor. J Neurochem. 2014;131:767-77.
- 651 36. Qi YX, Jin M, Ni XY, Ye GY, Lee Y, Huang J. Characterization of three serotonin receptors
652 from the small white butterfly, *Pieris rapae*. Insect Biochem. Mol. Biol. 2017;87:107-16.
- 653 37. Thamm M, Balfanz S, Scheiner R, Baumann A, Blenau W. Characterization of the 5-HT_{1A}
654 receptor of the honeybee (*Apis mellifera*) and involvement of serotonin in phototactic
655 behavior. Cell Mol. Life Sci. 2010;67:2467-79.
- 656 38. Schlenstedt J, Balfanz S, Baumann A, Blenau W. Am5-HT₇: molecular and pharmacological
657 characterization of the first serotonin receptor of the honeybee (*Apis mellifera*). J
658 Neurochem. 2006;98:1985-98.
- 659 39. Berridge MJ, Patel N. Insect salivary glands - stimulation of fluid secretion by 5-
660 hydroxytryptamine and adenosine-3', 5'-monophosphate. Science. 1968;162:462-3.
- 661 40. Berridge MJ. The role of 5-hydroxytryptamine and cyclic AMP in the control of fluid
662 secretion by isolated salivary glands. J Exp Biol. 1970;53:171-86.
- 663 41. Vanhoenacker P, Haegeman G, Leysen JE. 5-HT₇ receptors: current knowledge and future

- 664 prospects. Trends Pharmacol. Sci. 2000;21:70-7.
- 665 42. Molaei G, Lange AB. The association of serotonin with the alimentary canal of the African
666 migratory locust, *Locusta migratoria*: distribution, physiology and pharmacological profile.
667 J Insect Physiol. 2003;49:1073-182.
- 668 43. Baines D, DeSantis T, Downer RGH. Octopamine and 5-hydroxytryptamine enhance the
669 phagocytic and nodule formation activities of cockroach (*Periplaneta americana*)
670 haemocytes. J Insect Physiol. 1992;38:905-14.
- 671 44. Kim K, Madanagapol N, Lee D, Ki Y. Octopamine and 5-hydroxytryptamine mediate
672 hemocytic phagocytosis and nodule formation via eicosanoids in the beet armyworm,
673 *Spodoptera exigua*. Arch. Insect Biochem. Physiol. 2009;90:162-76.
- 674 45. Kim GS, Kim Y. Up-regulation of circulating hemocyte population in response to bacterial
675 challenge is mediated by octopamine and 5-hydroxytryptamine via Rac1 signal in
676 *Spodoptera exigua*. J. Insect Physiol. 2010;56:559-66.
- 677 46. Kim Y, Ji D, Cho S, Park Y. Two groups of entomopathogenic bacteria, *Photorhabdus* and
678 *Xenorhabdus*, share an inhibitory action against phospholipase A₂ to induce host
679 immunodepression. J Invertebr Pathol. 2005;89: 258-64.
- 680 47. Shi YM, Bode HB. Chemical language and warfare of bacterial natural products in bacteria-
681 nematode-insect interactions. Nat Prod Rep 2018;35:309-35.
- 682 48. Tobias NJ, Shi YM, Bode HB. Refining the natural product repertoire in entomopathogenic
683 bacteria. Trends Microbiol. 2018;26:833-40.
- 684 49. Barak LS, Tiberi M, Freedman NJ, Kwatra MM, Lefkowitz RJ, Caron MG. A highly
685 conserved tyrosine residue in G protein-coupled receptors is required for agonist-mediated
686 β 2-adrenergic receptor sequestration. J Biol Chem 1994;269:2790-5.

- 687 50. Ji TH, Grossmann M, Ji I. G protein-coupled receptors. I. Diversity of receptor-ligand
688 interactions. *J Biol Chem.* 1998;273:17299-302.
- 689 51. Huang ES. Construction of a sequence motif characteristic of aminergic G protein-coupled
690 receptors. *Protein Sci.* 2003;12:1360-67.
- 691 52. Park J, Stanley D, Kim Y. Rac1 mediates cytokine-stimulated hemocyte spreading via
692 prostaglandin biosynthesis in the beet armyworm, *Spodoptera exigua*. *J Insect Physiol.*
693 2013;59:682-9.
- 694 53. Venkatakrisnan AJ, Deupi X, Lebon G, Tate CG, Schertler GF, Babu MM. Molecular
695 signatures of G-protein-coupled receptors. *Nature* 2013;494:185-94.
- 696 54. Ho BY, Karschin A, Branchek T, Davidson N, Lester HA. The role of conserved aspartate
697 and serine residues in ligand binding and in function of the 5-HT_{1A} receptor: A site-directed
698 mutation study. *FEBS Lett.* 1992;312:259-62.
- 699 55. Shapiro DA, Kristiansen K, Weiner DM, Kroeze WK, Roth BL. Evidence for a model of
700 agonist-induced activation of 5-hydroxytryptamine 2A serotonin receptors that involves the
701 disruption of a strong ionic interaction between helices 3 and 6. *J. Biol. Chem.*
702 2002;277:11441-9.
- 703 56. Qanbar R, Bouvier M. Role of palmitoylation/depalmitoylation reactions in G-protein-
704 coupled receptor function. *Pharmacol. Ther.* 2003;97:1-33.
- 705 57. Romero G, von Zastrow M, Friedman PA. Role of PDZ proteins in regulating trafficking,
706 signaling, and function of GPCRs: means, motif, and opportunity. *Adv Pharmacol.*
707 2011;62:279-314.
- 708 58. Guseva D, Wirth A, Ponimaskin E. Cellular mechanisms of the 5-HT₇ receptor-mediated
709 signaling. *Front. Behav. Neurosci.* 2014;8:306.

- 710 59. Choi C, Helfman DM. The Ras-ERK pathway modulates cytoskeleton organization, cell
711 motility and lung metastasis signature genes in MDA-MB-231 LM2. *Oncogene*
712 2014;33:3668-76.
- 713 60. Papenfort K, Bassler BL. Quorum sensing signal-response systems in Gram-negative bacteria.
714 *Nat. Rev. Microbiol.* 2016;14:576-88.
- 715 61. Bode E, He Y, Vo TD, Schultz R, Kaiser M, Bode HB. Biosynthesis and function of simple
716 amides in *Xenorhabdus doucetiae*. *Environ. Microbiol.* 2017;19:4564-75.
- 717 62. Reimer D, Nollmann FI, Schultz K, Kaiser M, Bode HB. Xenortide biosynthesis by
718 entomopathogenic *Xenorhabdus nematophila*. *J Nat Prod.* 2014;77:1976-80.
- 719 63. Bloudoff K, Schmeing TM. Structural and functional aspects of the nonribosomal peptide
720 synthetase condensation domain superfamily: discovery, dissection and diversity. *Biochim*
721 *Biophys Acta* 2017;1865:1587-604.
- 722 64. Proschak A, Zhou Q, Schöner T, Thanwisai A, Kresovic D, Dowling A, et al. Biosynthesis of
723 the insecticidal xenocycloins in *Xenorhabdus bovienii*. *Chembiochem.* 2014;15:369-72.
- 724 65. Li J, Chen G, Webster JM. Nematophin, a novel antimicrobial substance produced by
725 *Xenorhabdus nematophilus* (Enterobacteriaceae). *Can J Microbiol.* 1997;43:770-3.
- 726 66. Nollmann FI, Dauth C, Mulley G, Kegler C, Kaiser M, Waterfield NR. et al. Insect-specific
727 production of new GameXPeptides in *Photorhabdus luminescens* TTO1, widespread natural
728 products in entomopathogenic bacteria. *Chembiochem.* 2015;16:205-8.
- 729 67. Cai M, Li Z, Fan F, Huang Q, Shao X, Song G. Design and synthesis of novel insecticides
730 based on the serotonergic ligand 1-[(4-Aminophenyl) ethyl]-4-[3-(trifluoromethyl) phenyl]
731 piperazine (PAPP). *J Agric Food Chem.* 2009;58:2624-9.
- 732 68. Verlinden H, Vleugels R, Broeck JV. Serotonin, serotonin receptors and their actions in

- 733 insects. Neurotransmitter. 2015;2:e314
- 734 69. Shrestha S, Stanley D, Kim Y. PGE₂ induces oenocytoid cell lysis via a G protein-coupled
735 receptor in the beet armyworm, *Spodoptera exigua*. J. Insect Physiol. 2011; 57:1568-76.
- 736 70. Bustin SA, Benes V, Garson JA, Hellemans J, Huggett J, Kubista M, et al. The MIQE
737 guidelines: minimum information for publication of quantitative real-time PCR experiments.
738 Clin. Chem. 2009;55:4.
- 739 71. SAS Institute. SAS/STAT user's guide. SAS Institute, Inc., Cary, NC. 1989.

740 **Figure captions**

741

742 **Fig. 1. Bioinformatics analysis of a novel 5-HTR₇ identified from *S. exigua* (Se-5HTR:**

743 **MH025798). (A) Phylogenetic analysis of 5HTRs. Amino acid sequences were retrieved from**

744 GenBank: Hs5HTR1D (NP_000855.1), Ss5HTR1D (NP_999323.1), Rn5HTR1D

745 (NP_036984.1), Oc5HTR1D (NP_001164624.1), NP_000854.1 Hs5HTR1B (NP_000854.1),

746 Dr5HTR1D (NP_001139158.1), Hs5HTR1F (NP_000857.1), Hs5HTR1E (NP_000856.1),

747 Cp5HTR1E (NP_001166222.1), Hs5HTR1A (NP_000515.2), Ap5HTR1B (ABY85411.1),

748 Ms5HTR (ABI33827.1), Pr5HTR1B (XP_022120028.1), Am5HTR1 (NP_001164579.1),

749 Dm5HTR1B (NP_001163201.2), Pa5HTR1 (CAX65666.1), Pr5HTR1A (XP_022129638.1),

750 Ap5HTR1A (ABY85410.1), Hs5HTR7 (P34969), Rn5HTR7 (P32305), Pr5HTR7

751 (AMQ67549.1), Am5HTR7 (NP_001071289.1), Dm5HTR7 (NP_524599.1), Ae5HTR7

752 (Q9GQ54), Hs5HTR4 (Q13639), Cp5HTR4 (O70528), Rn5HTR4 (Q62758), Mm5HTR4

753 (P97288), Hs5HTR6 (P50406), Pt5HTR6 (Q5IS65), It5HTR6 (XP_005317590.1), Rn5HTR6

754 (P31388), Mm5HTR6 (Q9R1C8), Cp5HTR6 (XP_003471412.1), Pm5HTR2A (KPJ17794.1),

755 Pr5HTR2A (XP_022112310.1), Bm5HTR2A (NP_001296483.1), Cl5HTR2A

756 (XP_014254278.1), Rp5HTr2B (AKQ13312.1), Mq5HTR2A (KOX78271.1), Am5HTr2B

757 (NP_001189389.1), Hs5HTR2A (NP_000612.1), Hs5HTR2C (NP_000859.1), Hs5HTR2B







758 (NP_000858.3), Pt5HTR2C (XP_015921531.1), Mp5HTR2C (XP_022169104.1), Am5HTr2A

759 (NP_001191178.1), Pr5HTR2C (XP_022122944.1), Ba5HTR2C (XP_023955125.1),

760 Rn5HTR5B (P35365), Mm5HTR5B (P31387), Hs5HTR5A (NP_076917.1), Rn5HTR5A

761 (P35364), Mm5HTR5A (P30966), Hs5HTR3C (NP_570126.2), Hs5HTR3E (NP_001243542.1),

762 Hs5HTR3D (NP_001157118.1), Hs5HTR3B (NP_006019.1), Rn5HTR3B (NP_071525.1),

763 Hs5HTR3A (AP35868.1), Cp5HTR3A (O70212), Rn5HTR3A (NP_077370.2), Mm5HTR3A
764 (P23979). The phylogenetic tree was constructed using neighbor-joining method. Bootstrap
765 values on branch nodes were obtained after 1,000 repetitions. **(B)** Amino acid sequence
766 alignment of *Se*-5HTR with orthologous receptors from *Homo sapiens* (Hs-5HTR7: P34969),
767 *Drosophila melanogaster* (Dm-5HTR7: NP_524599.1), *Manduca sexta* (Ms-5HTR7:
768 AGL46976.1), and *Pieris rapae* (Pr-5HTR7: AMQ67549.1). Identical residues among these five
769 sequences are illustrated as white letters against black. Dashes within sequences indicate gaps
770 introduced to maximize homology. Putative seven transmembrane domains (TM1-TM7) are
771 shown as blue bars. Potential N-glycosylation sites () , potential phosphorylation sites for
772 protein kinase A and/or C () , potential residue to interact with 5-HT amino group () and 5-
773 HT hydroxyl group () , potential disulfide bond groups () , and potential post translational
774 palmitoylation sites () are indicated. Overbars indicate unique motif to aminergic receptor,
775 agonist mediated sequestration and resensitization motif, and PDZ-domain binding motif,
776 respectively. Conserved domains were determined using InterPro tool
777 (<https://www.ebi.ac.uk/interpro/>) and Prosite (<http://prosite.expasy.org/>) whereas other residues
778 and motifs were predicted using several tools from DTU bioinformatics
779 (www.cbs.dtu.dk/services/).

780
781 **Fig. 2. Expression profile of *Se*-5HTR.** **(A)** Differential expression of *Se*-5HTR in different
782 developmental stages: egg, larval instars ('L1-L5'), pupa ('Pu'), and adult ('Ad'). **(B)**
783 Differential expression of *Se*-5HTR in different tissues of L5 larvae: hemocyte ('HC'), midgut
784 ('GUT'), fat body ('FB'), and brain ('BR'). **(C)** Expression pattern of *Se*-5HTR in immune-
785 challenged L5 larvae: *Escherichia coli* ('Ec'), *Xenorhabdus nematophila* ('Xn'), *Photorhabdus*

786 *temperata temperata* ('Ptt'), *Serratia marcescens* ('Sm'), and *Beauveria bassiana* ('Bb').
787 Immune challenge was performed by injecting each L5 larva with 1.8×10^5 cells of bacteria or 5
788 $\times 10^5$ conidia of fungi. After incubation at 25°C for 8 h, gene expression analysis was performed
789 using RT-PCR and RT-qPCR. As a constitutive expressional control, a ribosomal gene, *RL32*,
790 was used for expression analysis in RT-PCR and RT-qPCR. Each measurement was replicated
791 three times with independent biological samples. Histogram bars annotated with the same letter
792 are not significantly different at Type I error = 0.05 (LSD test).

793
794 **Fig. 3. Effect of an inhibitor specific to 5-HT₇ receptor ('SB-269970') on hemocyte**
795 **behaviors of *S. exigua*.** (A) Total hemocyte count (THC) analysis in L5 larvae. For the assay, 2
796 μg of 5-HT or 2 μg of SB-269970 was injected. THC was assessed with or without bacterial co-
797 injection (1.8×10^5 cells per larva). (B) Hemocyte-spreading behavior analysis. Hemocyte-
798 spreading was assessed with a 20 μL reaction mixture containing 1 or 2 μL test chemical with 18
799 or 19 μL hemocytes. 5-HT was co-applied with SB-269970 at ratios of 1:10 (2 μg 5-HT: 20 μg
800 SB-269970) and 10:1 (20 μg 5-HT: 2 μg SB-269970). Spread cells were stained with F-actin and
801 FITC-labeled phalloidin. Nuclei were stained with DAPI. Each treatment was independently
802 replicated three times. Histogram bars indicate percentages of spread hemocytes and error bars
803 indicate standard deviation. Histogram bars annotated with the same letter are not significantly
804 different at Type I error = 0.05 (LSD test).

805
806 **Fig. 4. RNA interference (RNAi) of *Se-5HTR* and suppression of hemocyte behaviors.** (A)
807 RNAi of *Se-5HTR* expression with a gene-specific dsRNA (dsSe-5HTR). About 900 ng of dsSe-
808 5HTR was injected to L5. At 0, 12, 24, and 48 h post-injection (PI), expression levels of *Se-*

809 *5HTR* were assessed from whole body. Expression levels of *Se-5HTR* in different tissue parts
810 were assessed at 24 h PI. As a constitutive expressional control, a ribosomal gene, *RL32*, was
811 used for expression analysis in RT-PCR and RT-qPCR. As a control RNAi (dsCON), dsRNA
812 specific to *CpBV-ORF302* (a viral gene) was used for expression analysis. In RT-qPCR, each
813 treatment was triplicated. **(B)** Influence of RNAi on up-regulation of total hemocyte count (THC)
814 in response to bacterial challenge. At 24 h PI of ds*Se-5HTR*, hemolymph was collected from L5
815 larvae for THC assessment. Each treatment was replicated three times. **(C)** Influence of RNAi on
816 hemocyte-spreading behavior. For spreading assay, hemocytes from larvae treated with dsRNA
817 were collected at 24 h. Each treatment was independently replicated three times. Spread cells
818 were stained with F-actin and FITC-labeled phalloidin. Nuclei were stained with DAPI.
819 Histogram bars indicate percentages of spread hemocytes and error bars indicate standard
820 deviation. Different letters above standard error bars indicate significant difference among means
821 at type I error = 0.05 (LSD test). Asterisks represent significant difference between control and
822 treatment in each tissue.

823

824 **Fig. 5. RNA interference (RNAi) of *Se-5HTR* and suppression of cellular immune responses.**

825 **(A)** Analysis of phagocytosis in L5 larvae of *S. exigua*. FITC-tagged *E. coli* were injected into
826 L5 larvae at 24 h post-injection of ds*Se-5HTR*. A specific inhibitor (SB-269970) to 5-HT₇
827 receptor was co-injected at a dose of 2 µg along with FITC-tagged bacteria. At 15 min after
828 injection, phagocytic cells were observed under a fluorescent microscope at 400 × magnification
829 and percentage of phagocytotic hemocytes was calculated from randomly chosen 100 cells. Total
830 hemocytes were observed from bright-field ('BF'). Each treatment was independently replicated
831 three times. **(B)** Nodulation assay. After RNAi, *E. coli* (1.8×10^5 cells/larva) was injected to L5

832 larvae. SB-269970 (2 µg/larva) was co-injected with bacteria. After 8 h incubation at 25°C,
833 treated insects were assessed for nodule formation. Histogram bars indicate percentages of
834 phagocytosis and error bars indicate standard deviation. Histogram bars annotated with the same
835 letter are not significantly different at Type I error = 0.05 (LSD test).

836

837 **Fig. 6. Immunosuppressive activities of organic extracts from culture broth of**
838 ***Xenorhabdus nematophila* ('Xn') and *Photorhabdus temperata temperata* ('Ptt') bacteria**
839 **against L5 larvae of *S. exigua*.** Each larva was injected with *E. coli* (10^5 cells) along with 1 µL
840 of ethyl acetate ('EAX') or butanol ('BX') extract. **(A)** Phagocytosis in L5 larvae. FITC-tagged
841 *E. coli* were injected to L5 larvae at 24 h post-injection of an organic extract. After 15 min,
842 phagocytic cells were observed under a fluorescent microscope at 400 × magnification and
843 percentage of phagocytotic hemocytes was calculated from randomly chosen 100 cells. Each
844 treatment was independently replicated three times. **(B)** Nodule formation. *E. coli* (1.8×10^5
845 cells/larva) was injected to L5 larvae. An organic extract was co-injected with the bacteria. After
846 8 h of incubation at 25°C, treated insects were assessed for nodule formation. Each treatment
847 was replicated with 10 larvae. Different letters above standard deviation bars indicate significant
848 difference among means at Type I error = 0.05 (LSD test).

849

850 **Fig. 7. Screening 37 bacterial secondary metabolites derived from *X. nematophila* and *P.***
851 ***temperata temperata* for their effects on cellular immune responses mediated by Se-5HTR in**
852 ***S. exigua*.** **(A)** Screening with phagocytosis assay. FITC-tagged *E. coli* cells were injected to L5
853 larvae along with 1 µg of each test chemical. After 15 min, phagocytic cells were observed under
854 a fluorescent microscope at 400 × magnification and percentage of phagocytotic hemocytes was

855 calculated from randomly chosen 100 cells. Each treatment was independently replicated three
856 times. **(B)** Screening with nodule formation assay. *E. coli* (1.8×10^5 cells/larva) was injected to
857 L5 larvae along with 1 μg of each test chemical. After 8 h of incubation at 25°C, treated insects
858 were assessed for nodule formation. Each treatment was replicated with 10 larvae. Asterisks
859 above standard deviation bars indicate significant difference compared to control ('CON'
860 without inhibitor) at Type I error = 0.05 (*), 0.01 (**), and 0.005 (***) (LSD test).

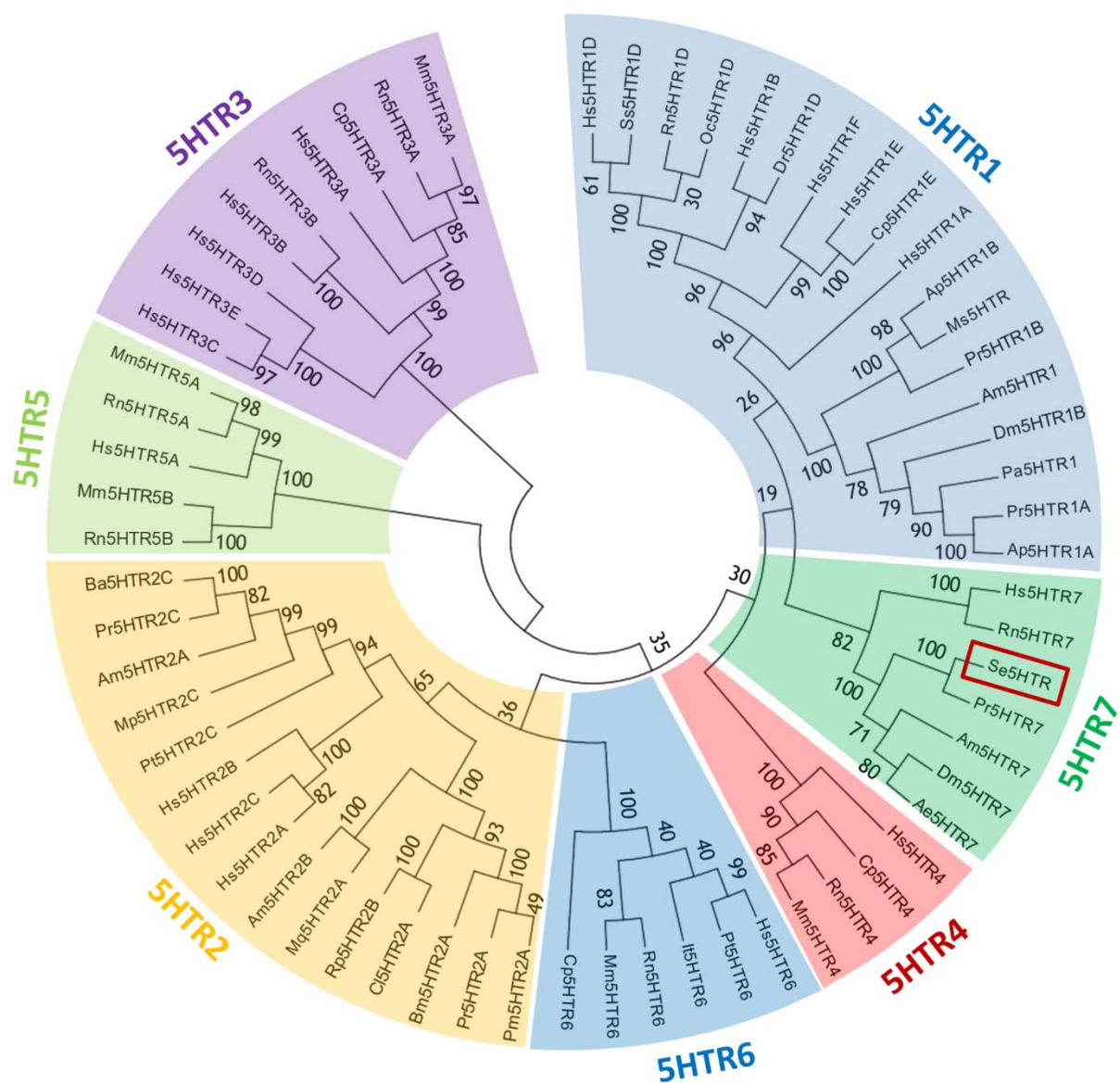
861
862 **Fig. 8. Competitive inhibition of 10 selected bacterial metabolites derived from *X.***
863 ***nematophila* and *P. temperata temperata* with 5-HT against Se-5HTR mediating**
864 **phagocytosis.** FITC-tagged *E. coli* cells were injected to L5 larvae along with test chemicals.
865 After 15 min, phagocytic cells were observed under a fluorescent microscope at $400 \times$
866 magnification and percentage of phagocytotic hemocytes was calculated from randomly chosen
867 100 cells. Each treatment was independently replicated three times. **(A)** Dose-response of
868 inhibitory compound (0, 0.01, 0.1, 1, and 10 $\mu\text{g/larva}$) with a fixed 5-HT concentration (1
869 $\mu\text{g/larva}$). **(B)** Dose-response of 5-HT (0, 0.02, 0.2, 2 and 20 $\mu\text{g/larva}$) with a fixed HB
870 compound concentration (1 $\mu\text{g/larva}$). 'CON' represents a positive control without any inhibitor.

871
872 **Fig. 9. Validation of phenylethylamide (PEA) compounds for their inhibitory activities**
873 **against 5-HTR using derivatives with different side chains ('X' and 'Y' of PEA skeleton).** **(A)**
874 Screening of 45 PEA derivatives for their effects on hemocyte phagocytosis of *S. exigua* with HB
875 44, a potent bacterial metabolite, as reference. PEA compounds (300 ng/larva) were injected into
876 hemocoels of L5 larvae along with FITC-tagged bacteria. After incubating for 15 min,
877 hemocytes were assessed for phagocytosis. Asterisks above standard deviation bars indicate

878 significant difference compared to control ('CON' without inhibitor) at Type I error = 0.05 (*),
879 0.01 (**), and 0.005 (***) (LSD test). **(B)** Chemical structures of three selected PEA compounds
880 and their median inhibitory doses (IC_{50}). **(C)** Competitive inhibition of the three selected PEA
881 derivatives with 5-HT against Se-5HTR mediated phagocytosis. For dose-response analysis of
882 inhibitory compounds (0, 0.3, 3, 30, and 300 ng/larva), a fixed 5-HT concentration (1 μ g/larva)
883 was used. For dose-response of 5-HT (0, 2, 20, 200 and 2,000 ng/larva), a fixed HB compound
884 concentration (1 μ g/larva) was used. 'CON' represents a positive control without any inhibitor.

885
886 **Fig. 10. Specific inhibition of a designed compound (PhX) on Se-5HTR with a commercial**
887 **5-HTR₇ inhibitor (SB-269970) as reference in phagocytosis of *S. exigua*.** FITC-tagged *E. coli*
888 cells were injected to L5 larvae along with test chemicals. After 15 min, phagocytic cells were
889 observed under a fluorescent microscope at 400 \times magnification and percentage of phagocytotic
890 hemocytes was calculated from randomly chosen 100 cells. Each treatment was independently
891 replicated three times. **(A)** Dose-response of PhX and SB-269970 with a fixed 5-HT
892 concentration (500 ng/larva). **(B)** Dose-response of 5-HT (0, 0.002, 0.02, 0.2, and 2 μ g/larva)
893 with a fixed inhibitor concentration (10 ng/larva). 'CON' represents a positive control without
894 any inhibitor.

(A)



(B)

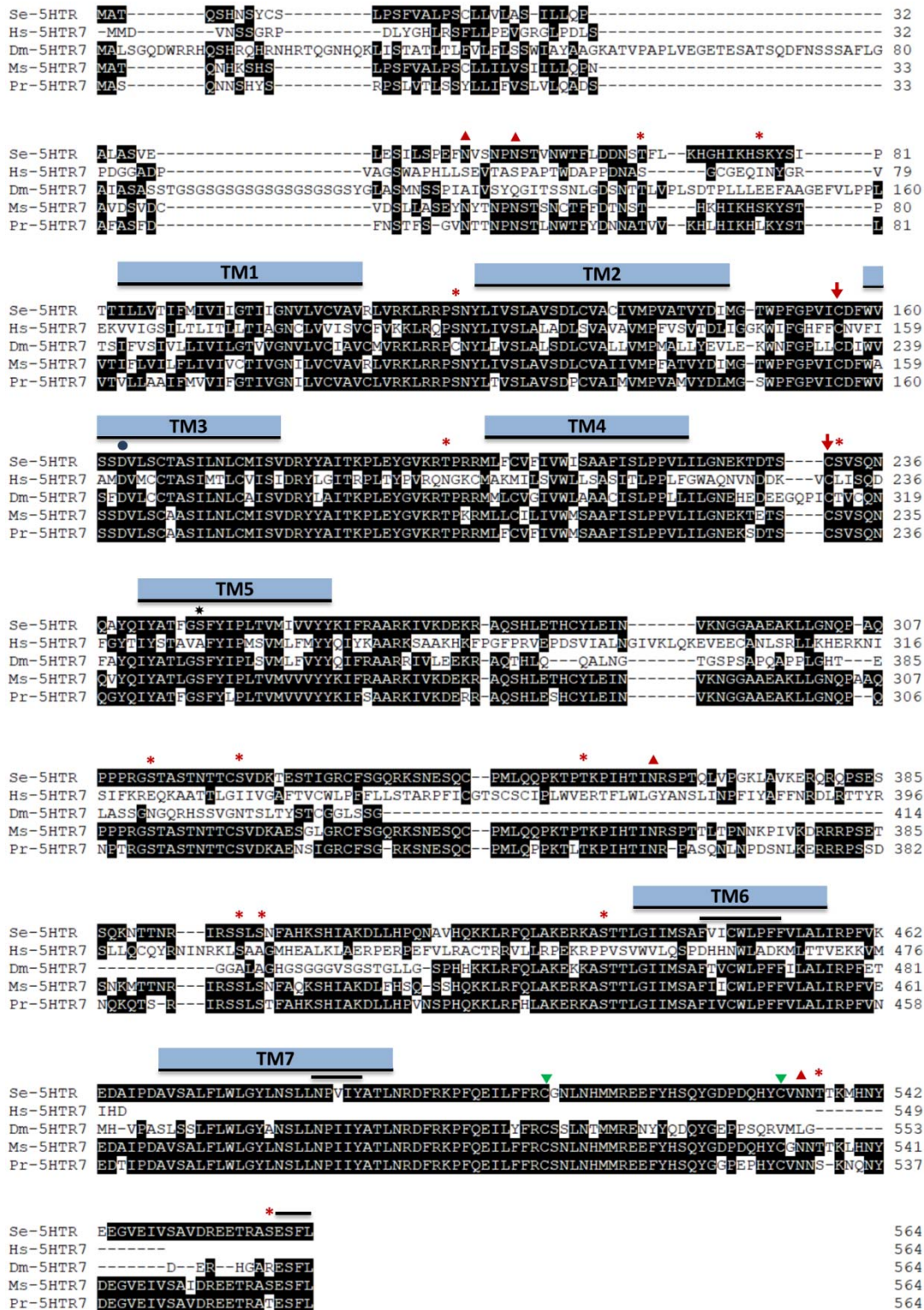


Fig. 1

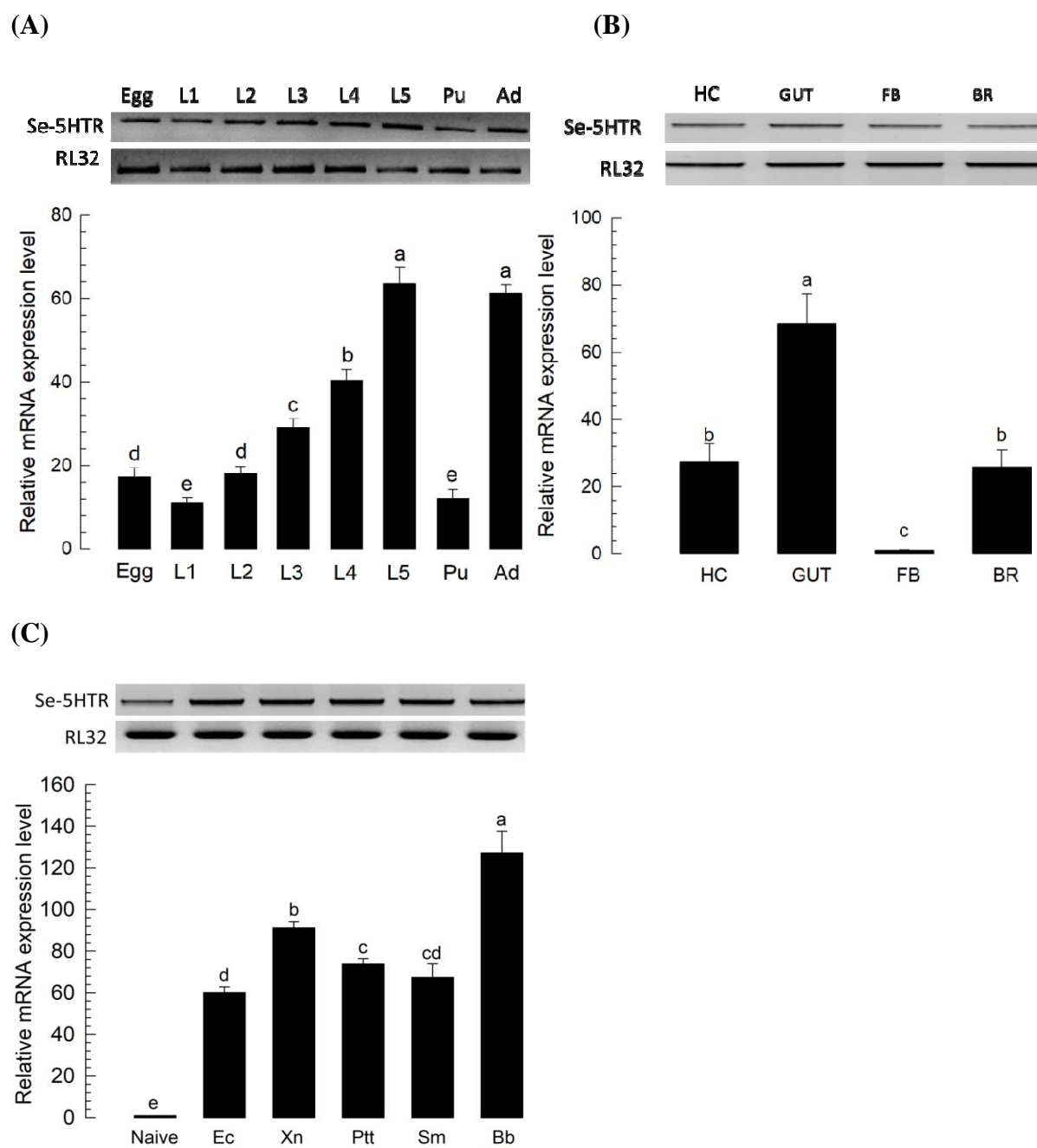
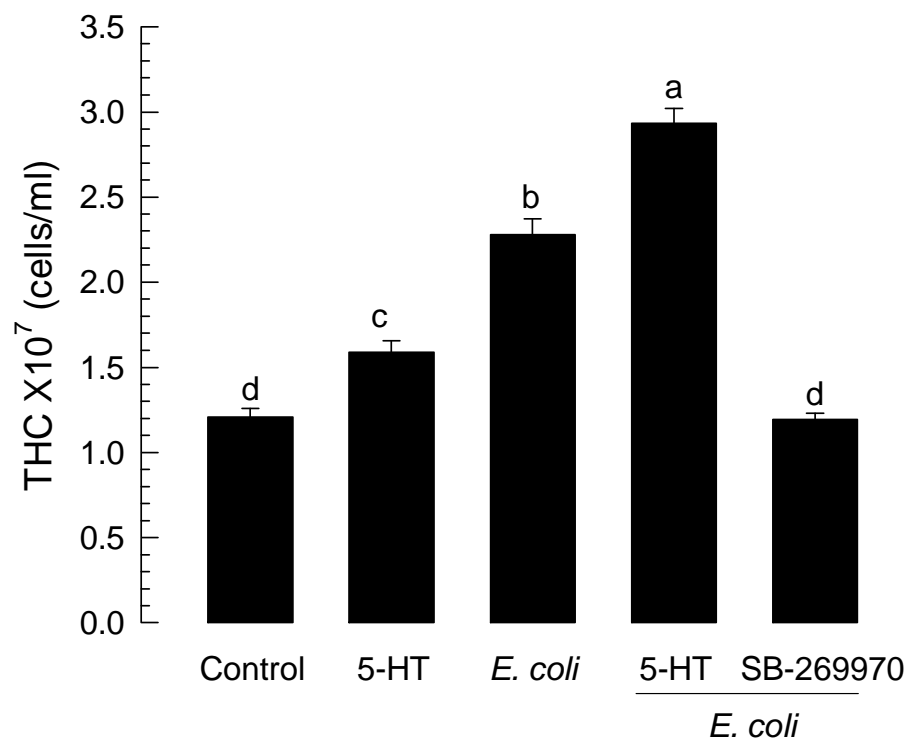


Fig. 2

(A)



(B)

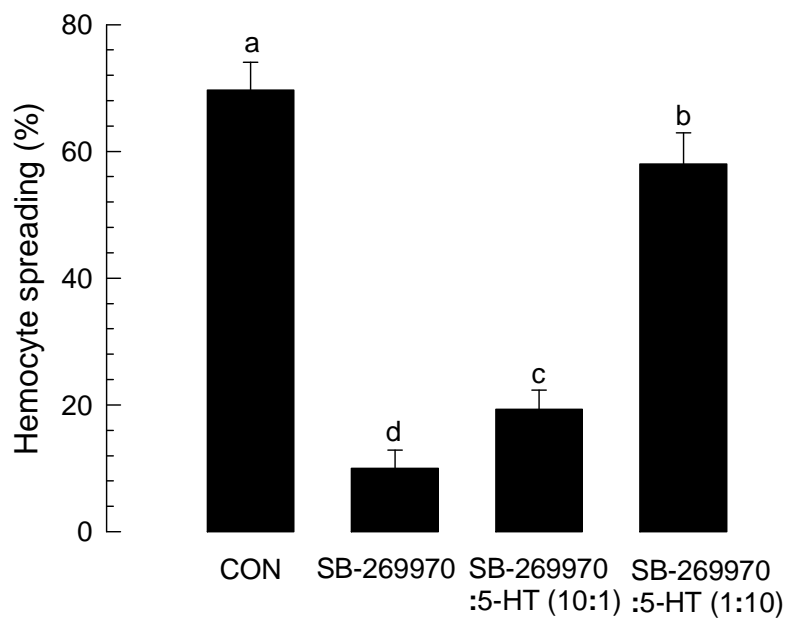
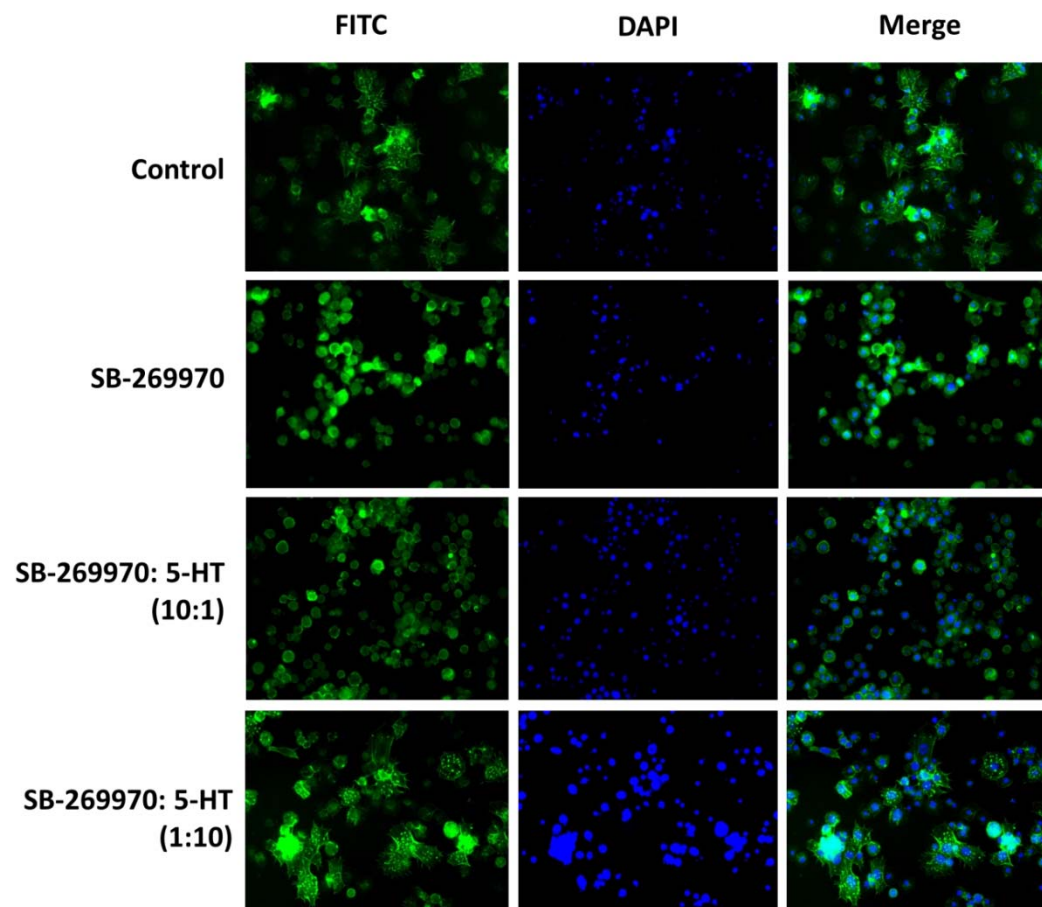
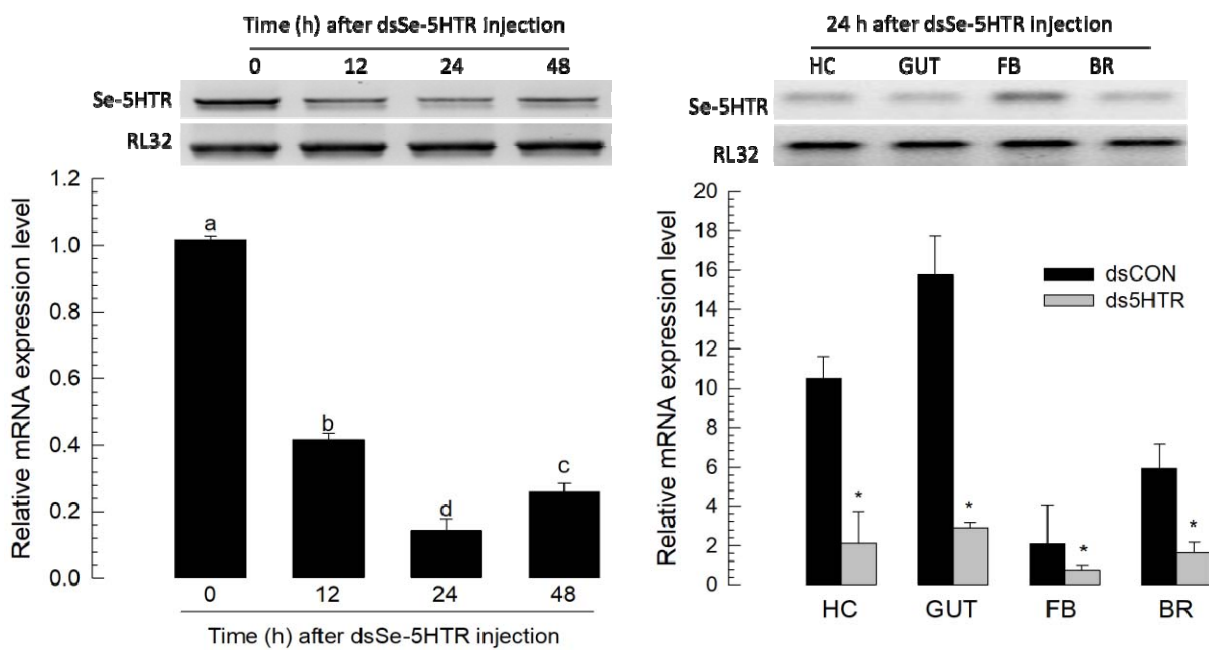
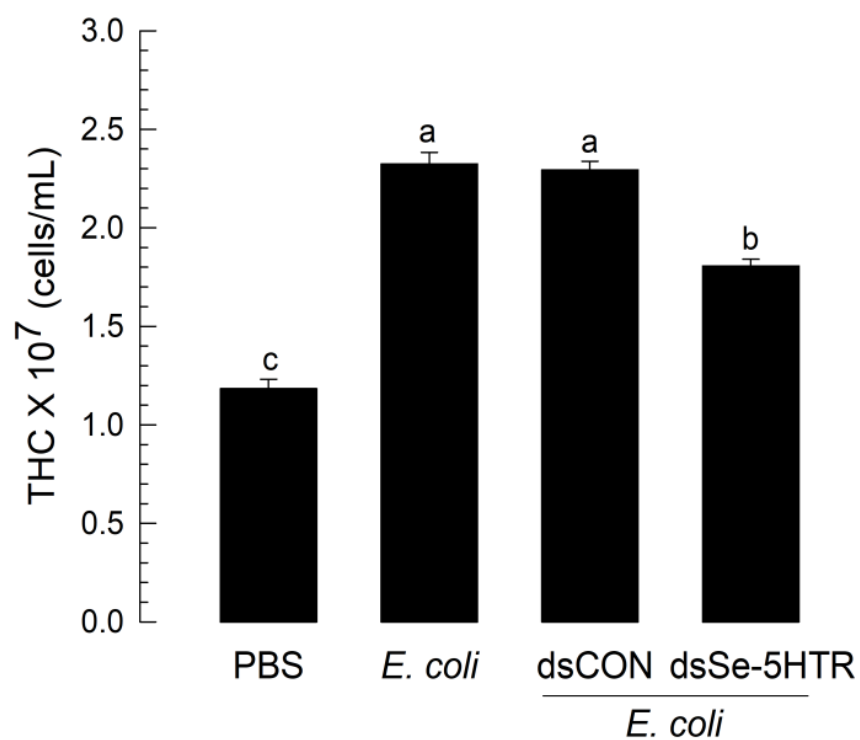


Fig. 3

(A)



(B)



(C)

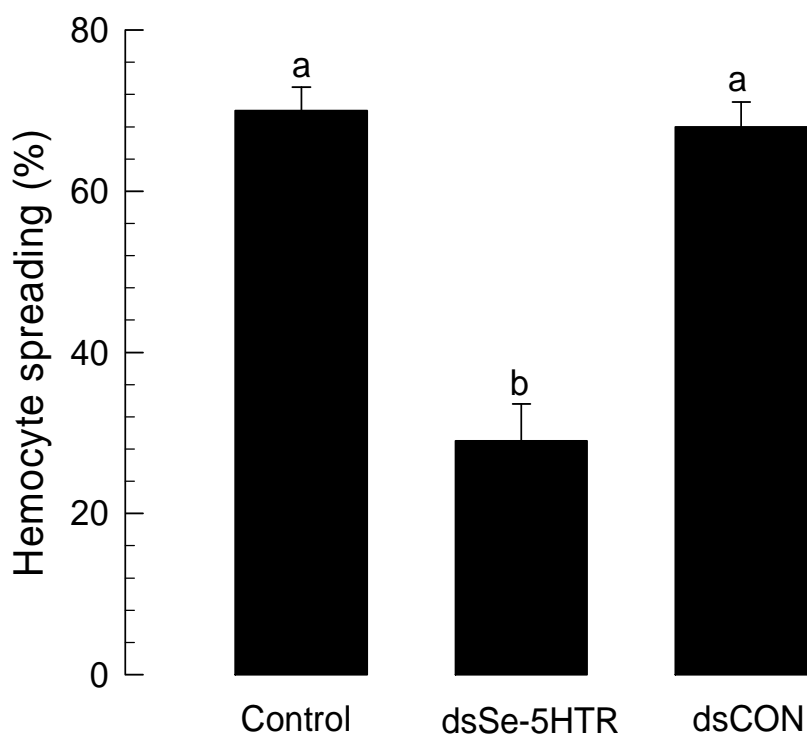
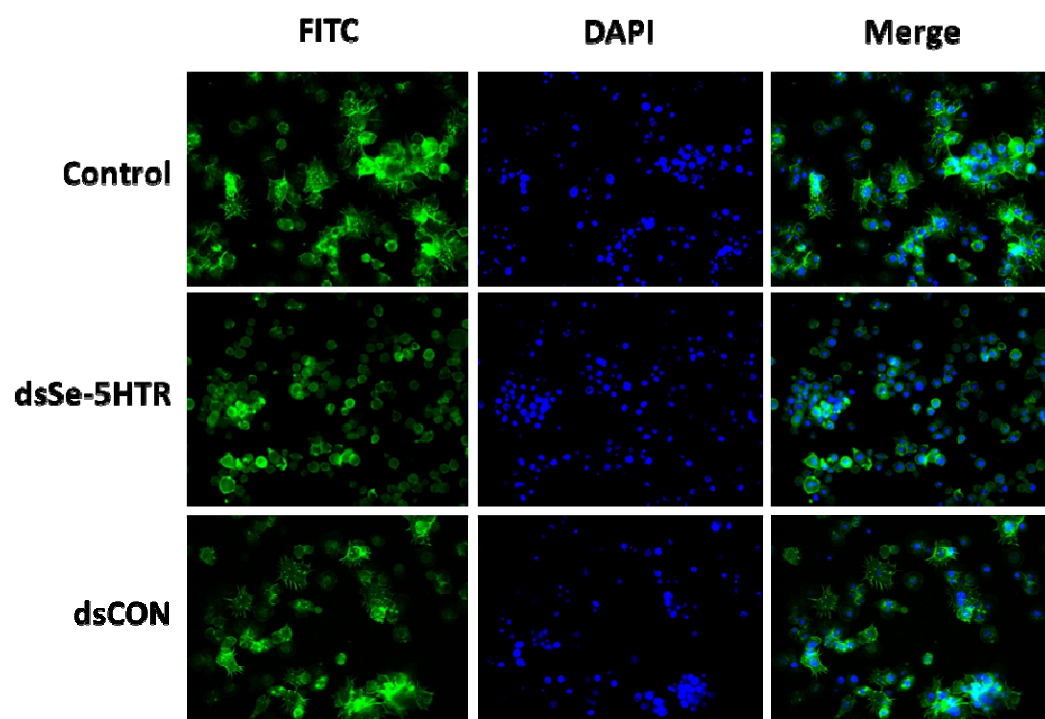
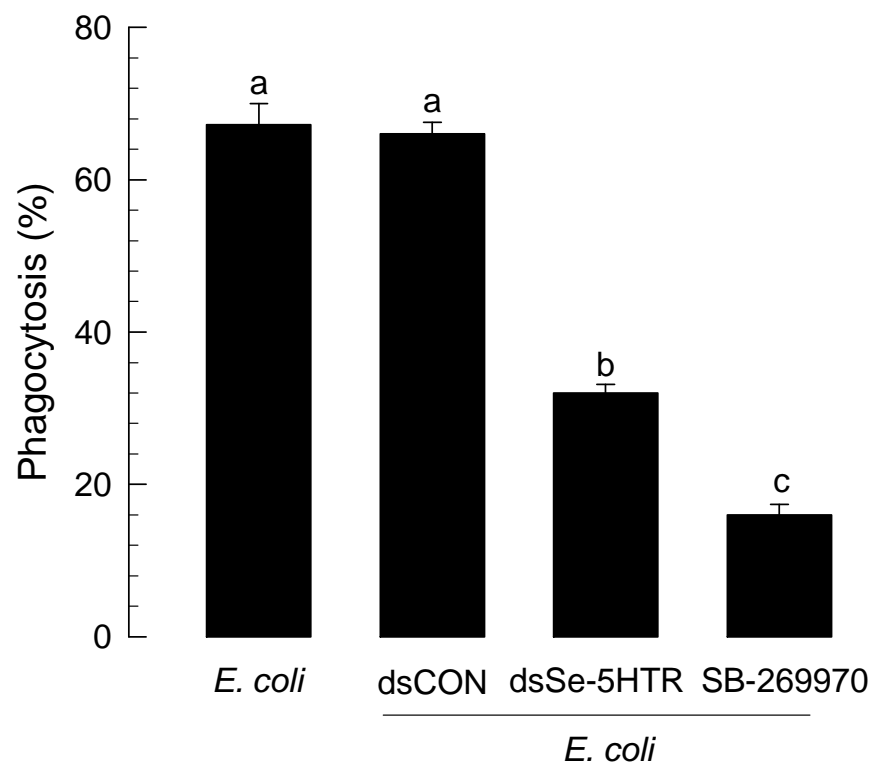
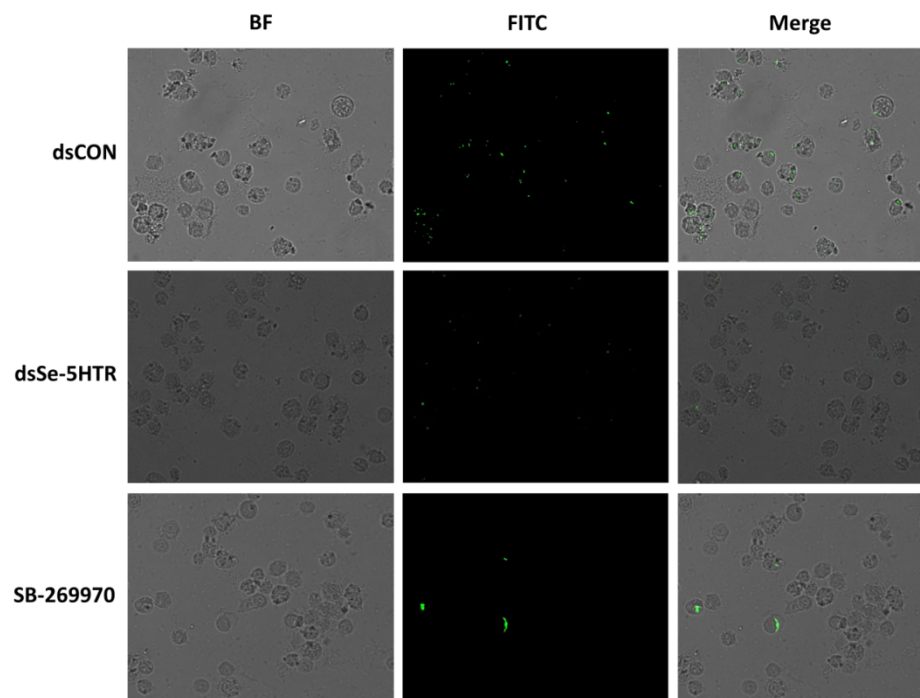


Fig. 4

(A)



(B)

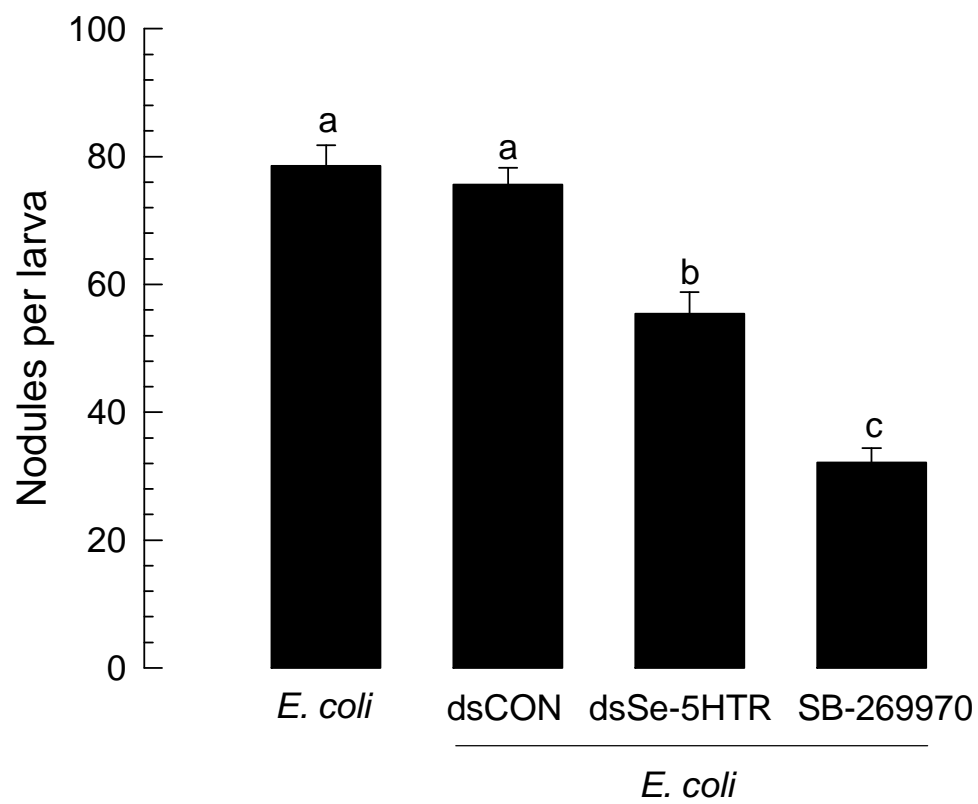
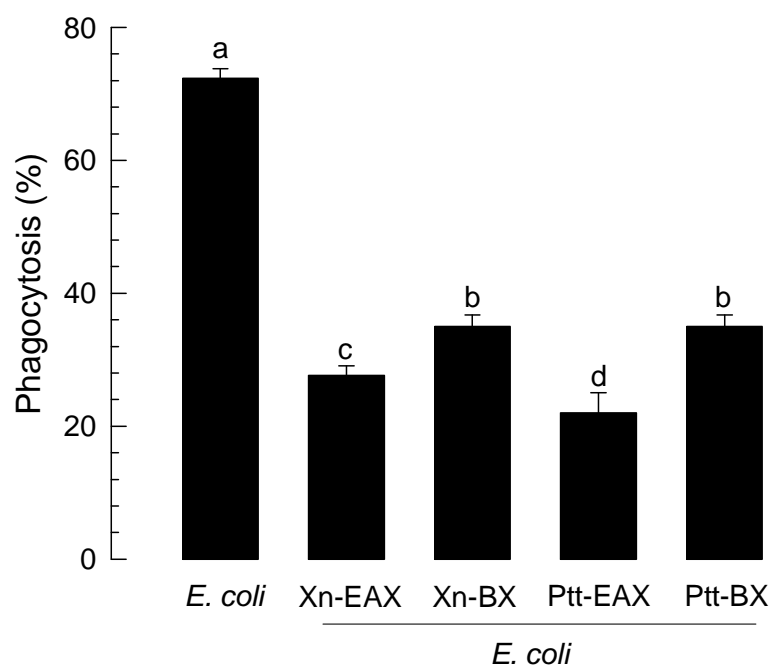


Fig. 5

(A)



(B)

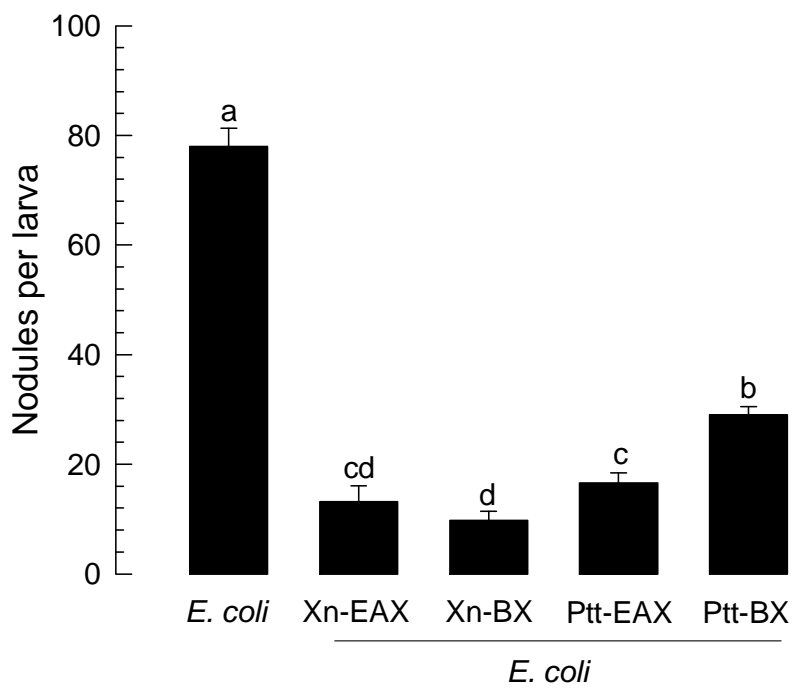


Fig. 6

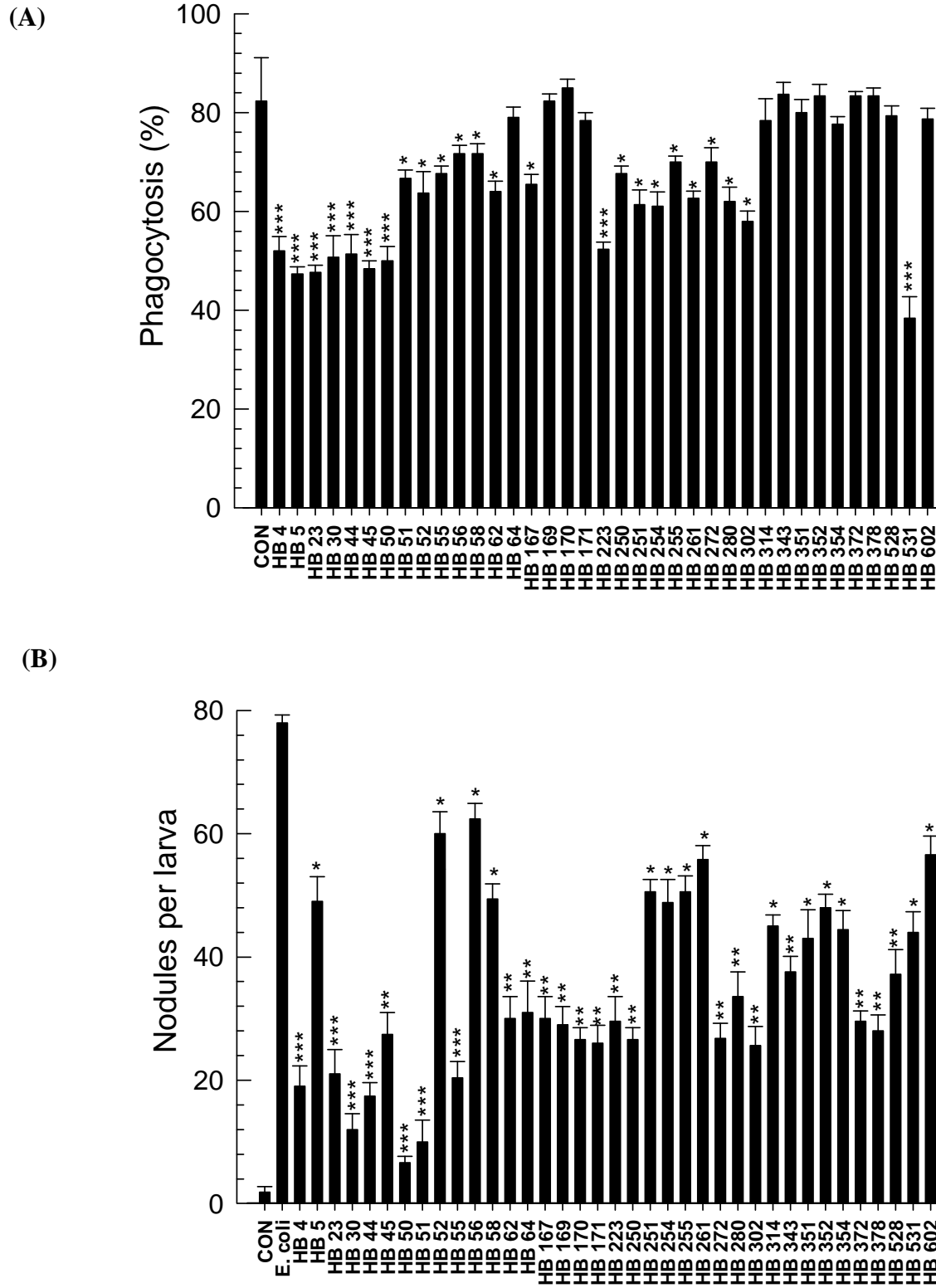
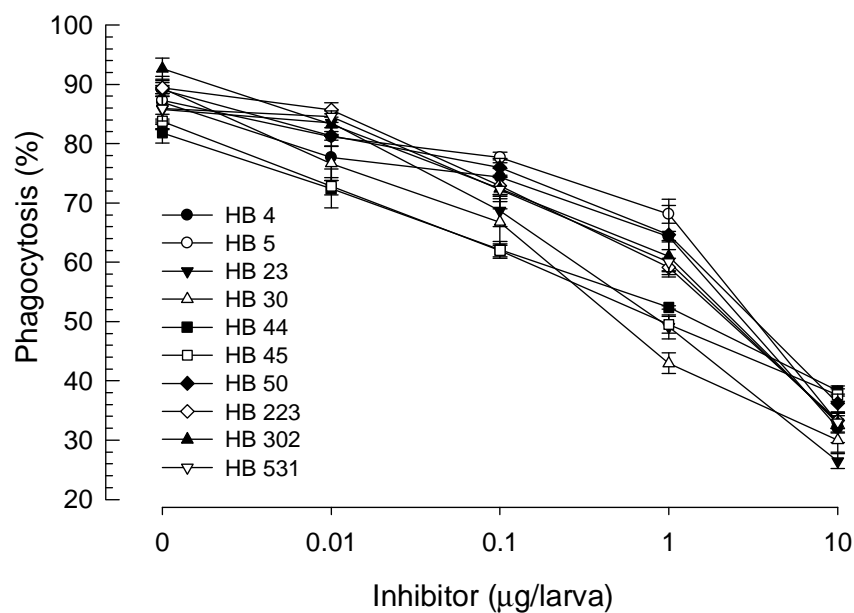


Fig. 7

(A)



(B)

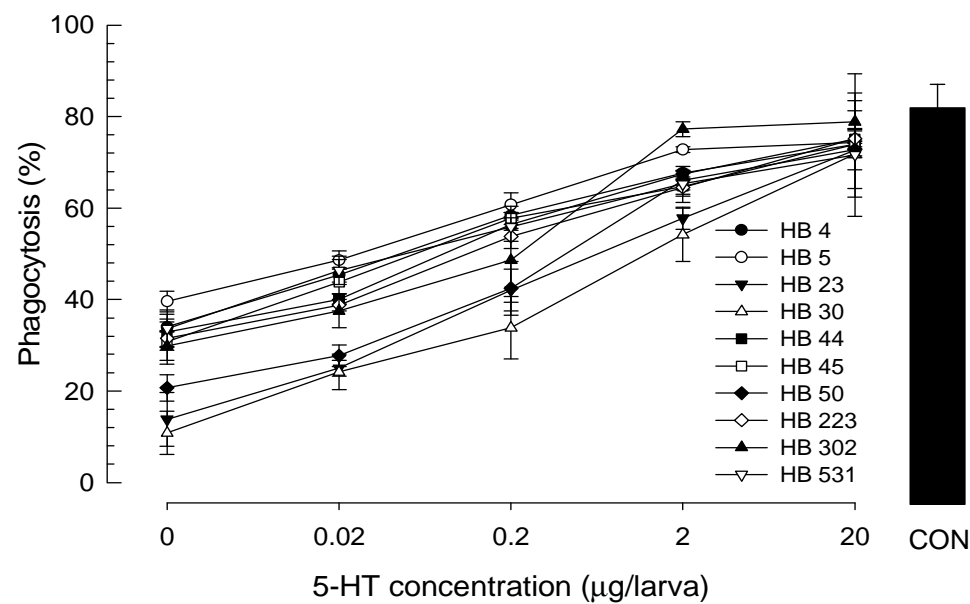
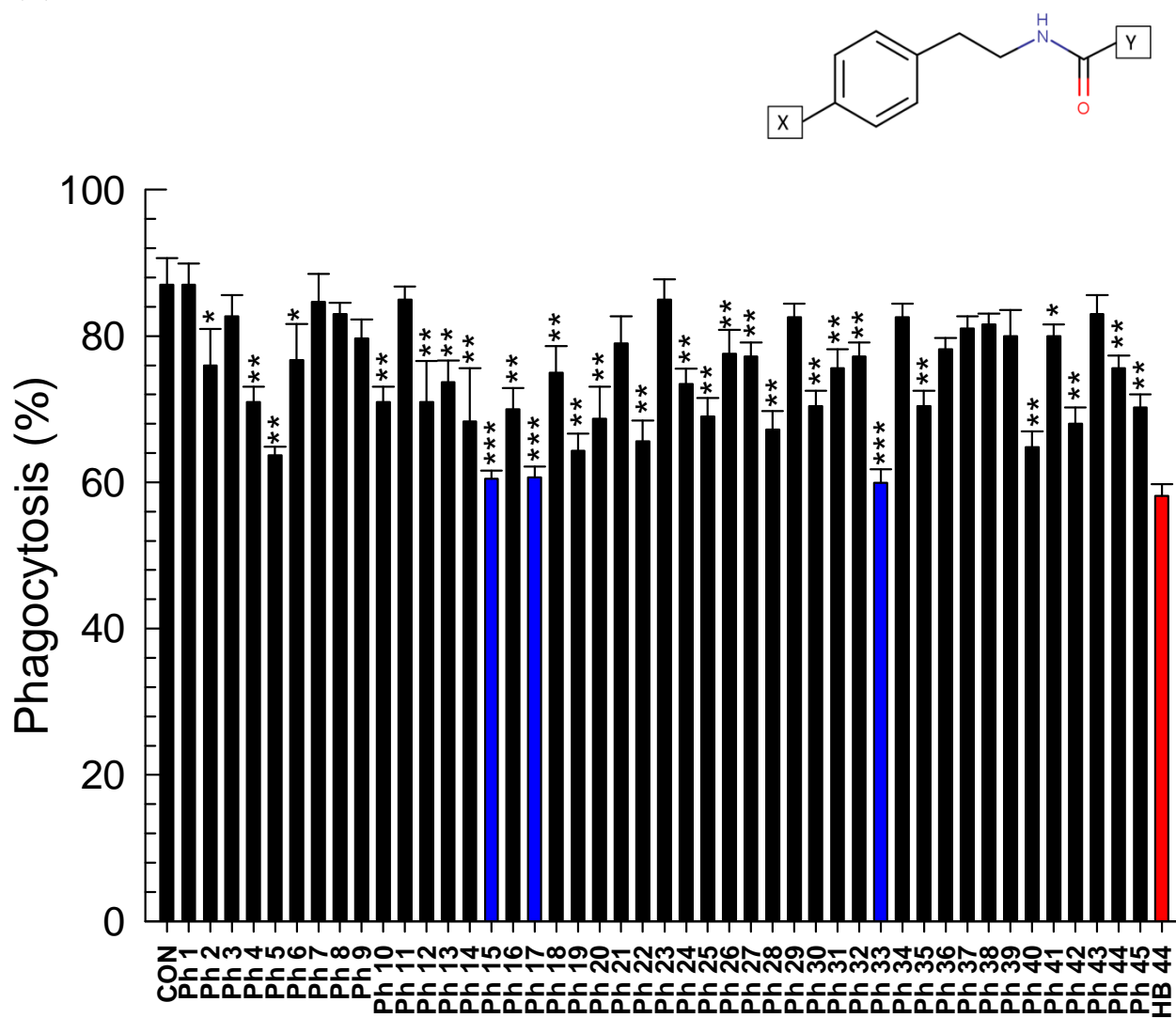


Fig. 8

(A)



(B)

Compound	Structure	IC ₅₀ (μM)
Ph 15		1.862 ± 0.221 ^c
Ph 17		2.746 ± 0.078 ^b
Ph 33		5.587 ± 0.98 ^a

(C)

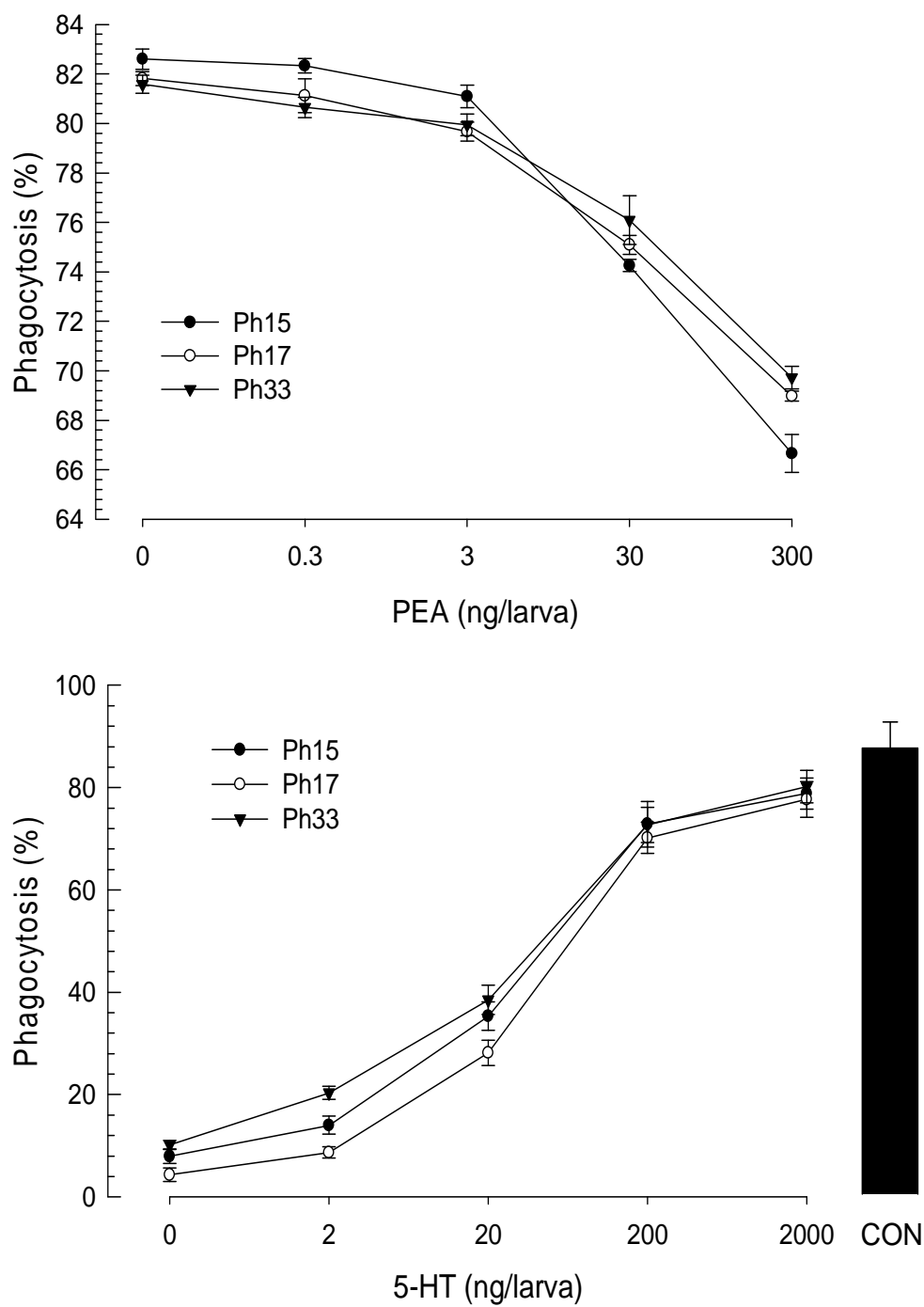


Fig. 9

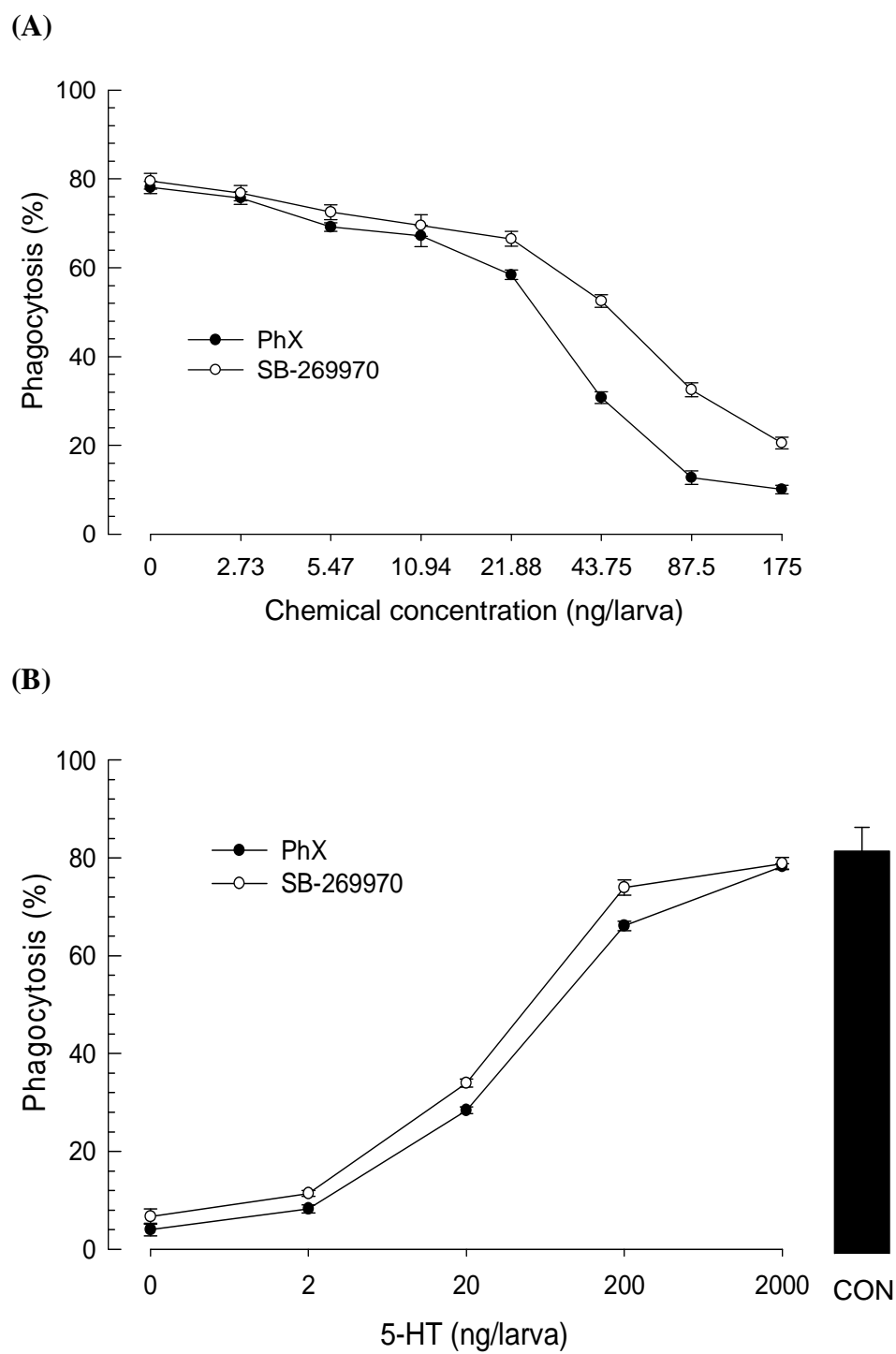


Fig. 10

Supplementary data

S1 Fig. Putative domain and motif structures of Se-5HTR. Putative seven transmembrane domains (TM1-TM7) are primarily marked by dark yellow bars and circles. Extracellular and cytosolic regions are denoted by green and light blue regions, respectively. Potential N-glycosylation sites and phosphorylation sites are marked by orange and red circles, respectively. Aspartic acid residue (dark blue circle) in TM3 and serine residue (light brown circle) in TM5 are putative residues that might chemically interact with 5-HT. The unique consensus sequence motif (PXXXWXPXF, dark brown circles) in aminergic receptors is conserved in TM6. The motif (NPXXY, dark blue circles) is conserved in TM7 like other GPCRs. Two possible post-translational palmitoylation cysteine residues (light yellow circles) and a PDZ-domain binding motif (ESFL, black circles) are also present in the C-terminal. Conserved motifs were determined using InterPro tool (<https://www.ebi.ac.uk/interpro/>) and Prosite (<http://prosite.expasy.org/>) whereas other residues and motifs were predicted using several tools from DTU bioinformatics.

S2 Fig. Potent screened chemicals from HB compounds with their chemical structures and respective median inhibitory concentrations (IC₅₀). HB chemicals were injected in different doses (0, 0.01, 0.1, 1, and 10 µg/larva) along with a fixed 5-HT concentration (1 µg/larva) and FITC-tagged bacteria (500 cells/larva). After 15 min of treatment, hemocytes from treated larvae were collected in ACB followed by phagocytosis assay as described above. Percentages of phagocytosis against HB chemical treatment with increasing concentrations were calculated. Their IC₅₀ values were determined using Probit analysis (<https://probitanalysis.wordpress.com>).

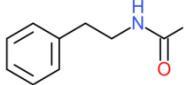
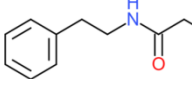
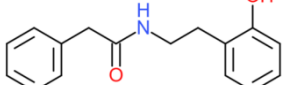
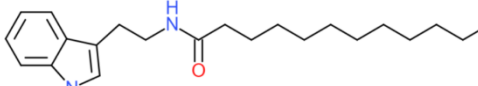
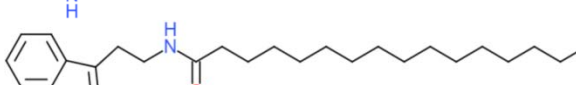
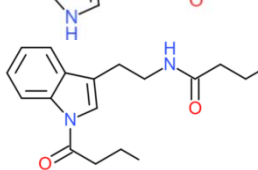
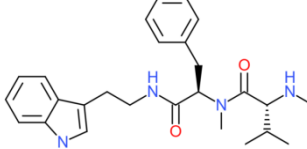
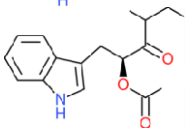
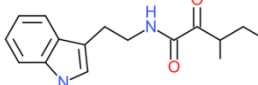
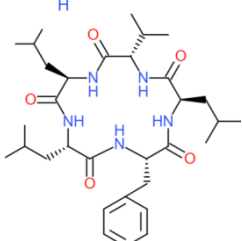
S3 Fig. Designing a potent chemical inhibitor from phenylethylamide (PEA) derivatives.

Derivatives of PEA were tested for their nodulation inhibition percentages and sorted by their X and Y groups. Most potent residues inhibiting nodulation were selected and a hypothetical most potent PEA chemical was designed. (A) Core PEA structure with two variable hypothetical residues (X and Y). X belongs to the residue group attached with para position of the phenyl ring whereas Y belongs to the residue group linked to the amide group. (B) Comparative analysis between X residue groups with their mean percent inhibition of nodulation. (C) Comparative analysis between Y residue groups with their percent inhibition of nodulation. (D) A hypothetical PEA chemical compound structure having the most potent inhibition capability.

S4 Fig. Bacterial secondary metabolites (37 chemicals) derived from *Xenorhabdus* and *Photorhabdus*

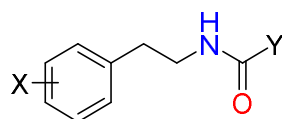
S5 Fig. Phenylethylamide (PEA) derivatives (45 chemicals) based on HB 44, a bacterial metabolite

S6 Fig. Chemical synthesis of PhX ((S)-2-(1,4-dioxohexahydropyrrolo[1,2-a]pyrazin-2(1H)-yl)-N-(4-methoxyphenethyl)acetamide)

Groups	ID	Structure	IC ₅₀ (μM)
Phenylethylamide	HB 4		253.2 ± 38.0
	HB 5		217.8 ± 43.6
	HB 44		103.7 ± 18.7
Tryptamide	HB 23		103.9 ± 15.6
	HB 50		90.6 ± 16.3
	HB 531		124.9 ± 23.7
Xenortide	HB 30		59.1 ± 9.5
Xenocylloin	HB 45		82.1 ± 14.8
Nematophin	HB 223		134.6 ± 22.9
GameXPepptide	HB 302		58.4 ± 11.7

S2 Fig

(A)



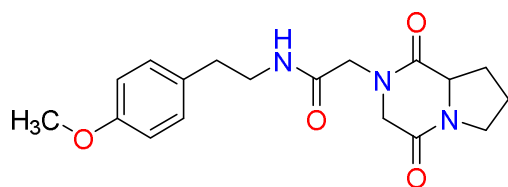
(B)

X	N	Inhibition of nodulation
4-OCH ₃	2	80.9%
3,4-di-OCH ₃	1	53.4%
4-Cl	3	49.6%
4-F	1	72.1%
4-CF ₃	1	66.9%
4-H	2	62.7%

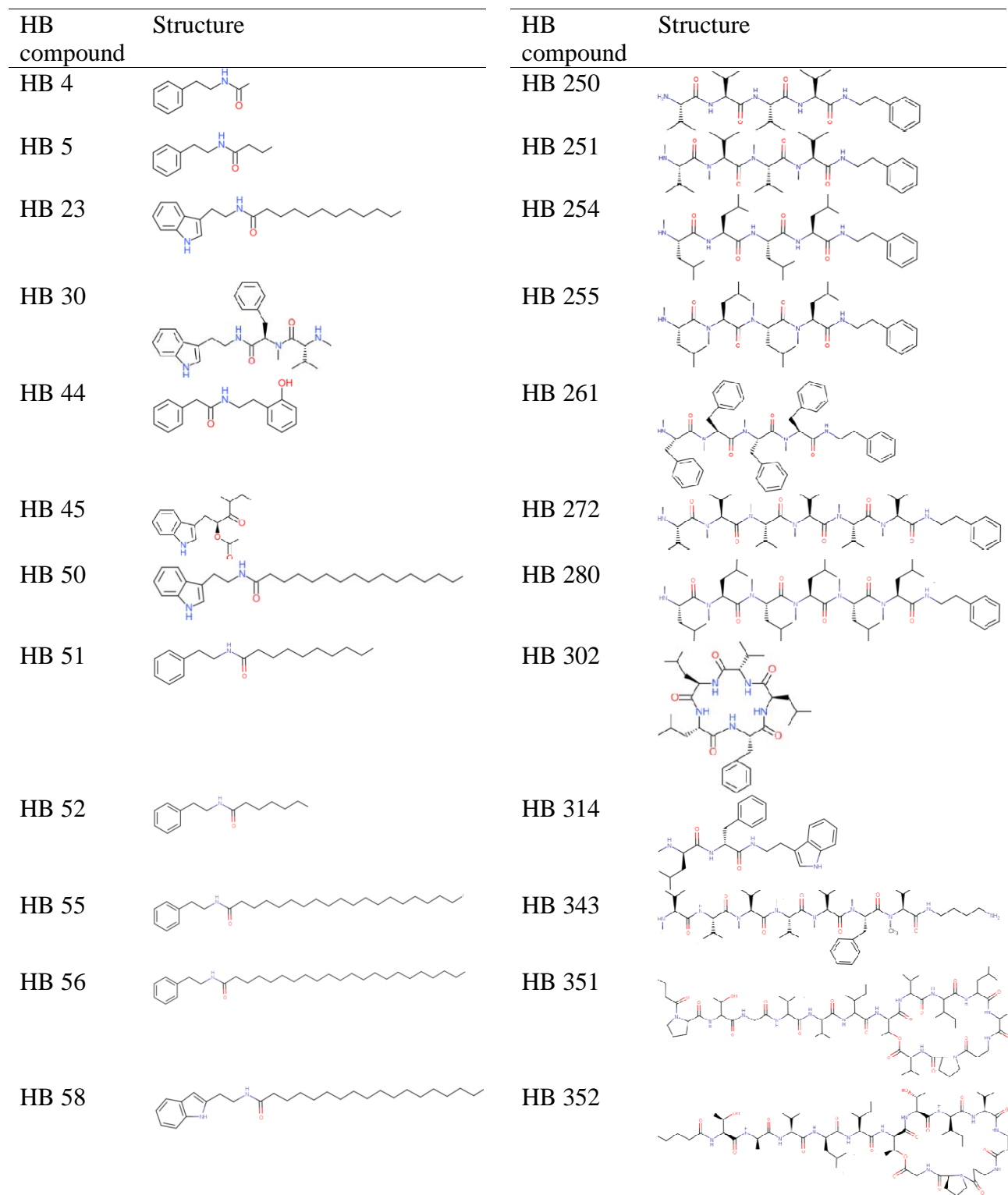
(C)

Y	Inhibition of nodulation
(X=4-Cl)	
	84.1%
	36.3%
	35.1%
(X=3,4-di-OMe)	
	77.7%
	77.3%
	53.4%
(X=4-F)	
	72.1%
(X=4-CF ₃)	
	66.9%
(X=4-H)	
	64.1%
	61.4%

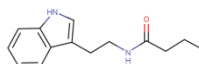
(D)



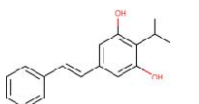
S3 Fig



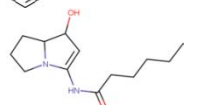
HB 62



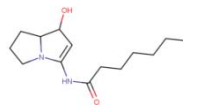
HB 64



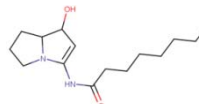
HB 167



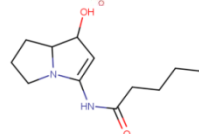
HB 169



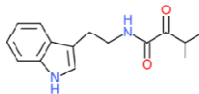
HB 170



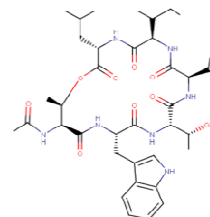
HB 171



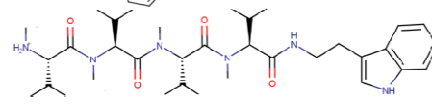
HB 223



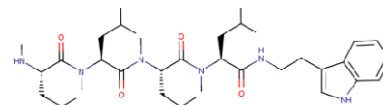
HB 354



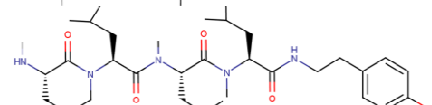
HB 372



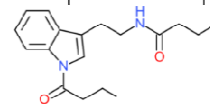
HB 378



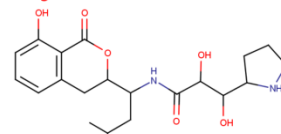
HB 528



HB 531

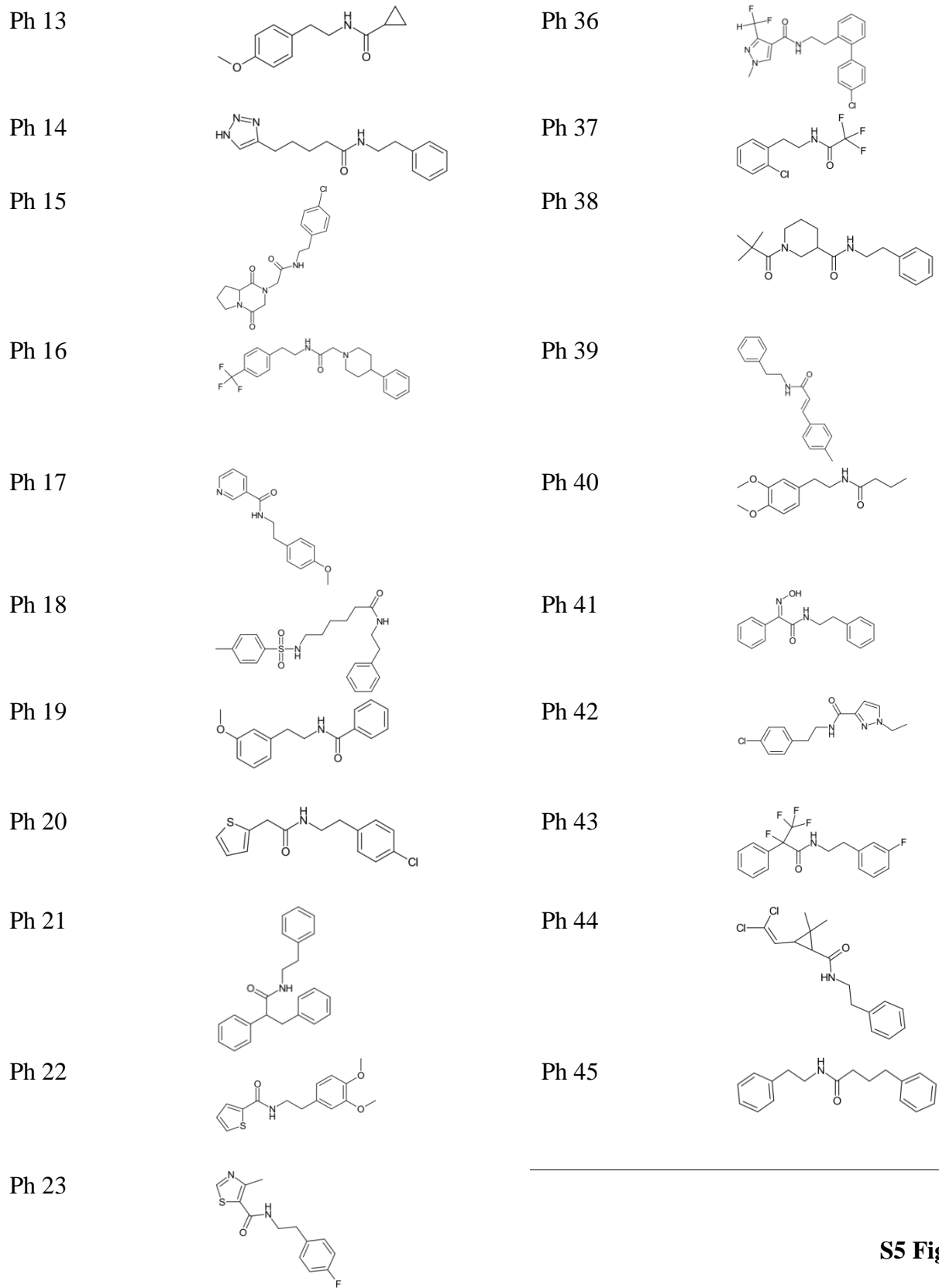


HB 602

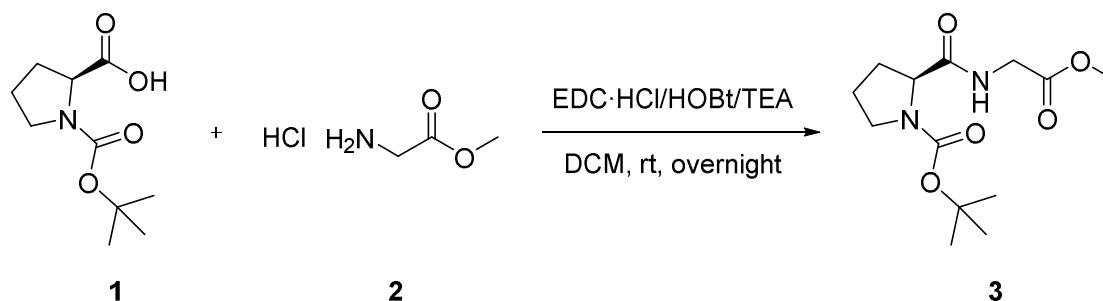


S4 Fig

PEA compound	Structure	PEA compound	Structure
Ph 1		Ph 24	
Ph 2		Ph 25	
Ph 3		Ph 26	
Ph 4		Ph 27	
Ph 5		Ph 28	
Ph 6		Ph 29	
Ph 7		Ph 30	
Ph 8		Ph 31	
Ph 9		Ph 32	
Ph 10		Ph 33	
Ph 11		Ph 34	
Ph 12		Ph 35	



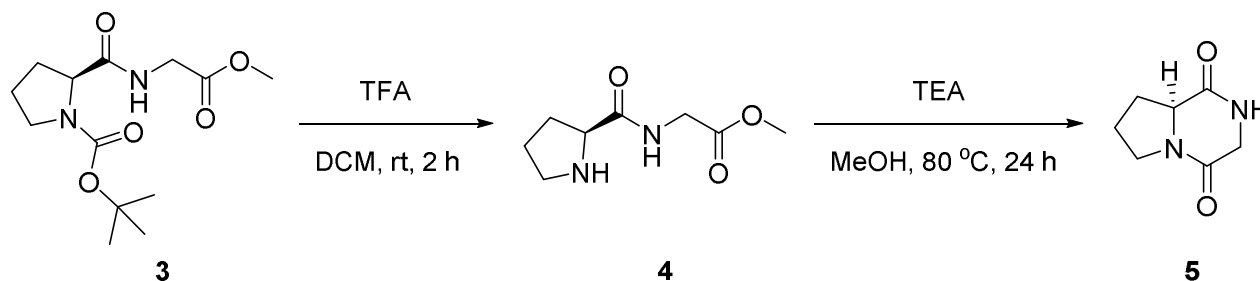
S5 Fig



Step 1

Synthesis of (*S*)-(-)-*N*-(*t*-butoxycarbonyl)-prolylglycine methylester (**3**)

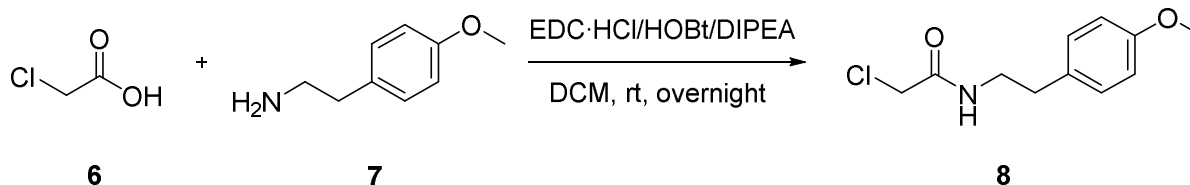
To a solution of (*S*)-(-)-*N*-(*t*-butoxycarbonyl)-proline **1** (5.00 g, 23.0 mmol) in CH₂Cl₂ (150 mL), amino acid methyl ester hydrochloride **2** (2.89 g, 23.0 mmol), 1-[3-(dimethylamino)propyl]-3-ethylcarbodiimide hydrochloride (5.34 g, 28.0 mmol), and 1-hydroxybenzotriazole monohydrate (3.77 g, 28.0 mmol) triethylamine (6.50 mL, 46.6 mmol) were added and the reaction mixture was stirred for 24 h at room temperature. The solvent was removed under reduced pressure. The residue was taken up in ethyl acetate (200 mL) and washed successively with water (200 mL), 1N HCl aqueous solution (200 mL), and sat. NaHCO₃ aqueous solution (200 mL). The solvent was removed under reduced pressure to give (*S*)-(-)-*N*-(*t*-butoxycarbonyl)-prolylglycine methylester **3** as a white solid (4.82 g, 73%).



Step 2

Synthesis of (*S*)-Hexahydropyrrolo[1,2-*a*]pyrazine-1,4-dione (**5**)

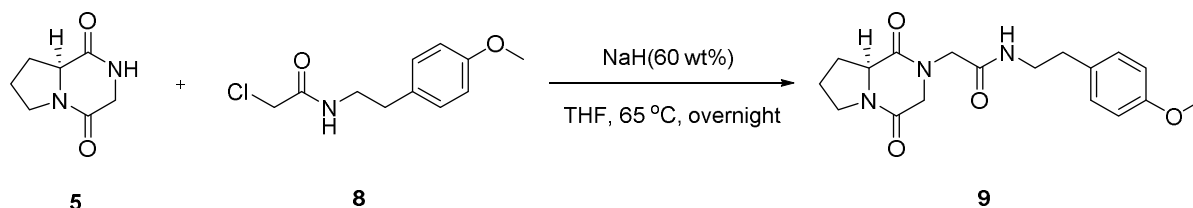
To a solution of (*S*)-(-)-*N*-(*t*-Butoxycarbonyl)-prolylglycine methylester **3** (4.80 g, 16.8 mmol) in CH₂Cl₂ (84 mL), trifluoroacetic acid (18.7 mL, 252.0 mmol) was added and the solution was stirred at room temp for 2 hr. The solvent was removed under reduced pressure. The residue was dissolved in MeOH (84 mL) and treated with triethylamine (9.3 mL, 67.2 mmol). The reaction mixture was kept under reflux overnight. The solvent was removed under reduced pressure and the oily residue was redissolved in *i*-propanol to give (*S*)-hexahydropyrrolo[1,2-*a*]pyrazine-1,4-dione **5** as a white solid (2.0 g, 78%).



Step 3

Synthesis of 2-chloro-*N*-(4-methoxyphenethyl)acetamide (**7**)

To a solution of 2-chloroacetic acid **6** (3.00 g, 31.8 mmol) in CH₂Cl₂ (160 mL), 2-(4-methoxyphenyl)ethylamine **7** (4.6 mL, 31.8 mmol) and *N,N*-diisopropylethylamine (8.45 mL, 63.5 mmol) were added and the reaction mixture was stirred for 15 min at room temperature. After addition of 1-[3-(dimethylamino)propyl]-3-ethylcarbodiimide hydrochloride (7.30 g, 38.1 mmol) and 1-hydroxybenzotriazole monohydrate (5.14 g, 38.1 mmol), the reaction mixture was stirred for 24 h at room temp. The reaction mixture was washed successively with 1 N HCl aqueous solution (160 mL) and sat. NaHCO₃ aqueous solution (160 mL). The organic layer was dried over MgSO₄, filtered, and concentrated. The residue was washed with diethyl ether to give 2-chloro-*N*-(4-methoxyphenethyl)acetamide **8** as a yellow solid (4.60 g, 63%).



Step 4

Synthesis of (*S*)-2-(1,4-dioxohexahydropyrrolo[1,2-*a*]pyrazin-2(*1H*)-yl)-*N*-(4-methoxyphenethyl)acetamide (**9**)

To a solution of (*S*)-hexahydropyrrolo[1,2-*a*]pyrazin-1,4-dione **5** (1.00 g, 6.40 mmol) in THF (32 mL), portionwise 60 wt% NaH (260 mg, 6.40 mmol) at 0°C was added and the reaction mixture was stirred 15 min at room temperature. 2-chloro-*N*-(4-methoxyphenethyl)acetamide **7** was added slowly to the reaction mixture then the mixture was stirred overnight at 65°C. The reaction was monitored by TLC. The reaction mixture was quenched with sat. NH₄Cl aqueous solution (100 mL) and extracted with EtOAc (2 X 100 mL). Combined organic layers were dried over MgSO₄, filtered, and concentrated. The crude product was purified by silica-gel column chromatography (eluent: MeOH 10% in CH₂Cl₂) to give (*S*)-2-(1,4-dioxohexahydropyrrolo[1,2-*a*]pyrazin-2(*1H*)-yl)-*N*-(4-methoxyphenethyl)acetamide **9** as a yellow foam (1.74 g, 79%).

S6 Fig